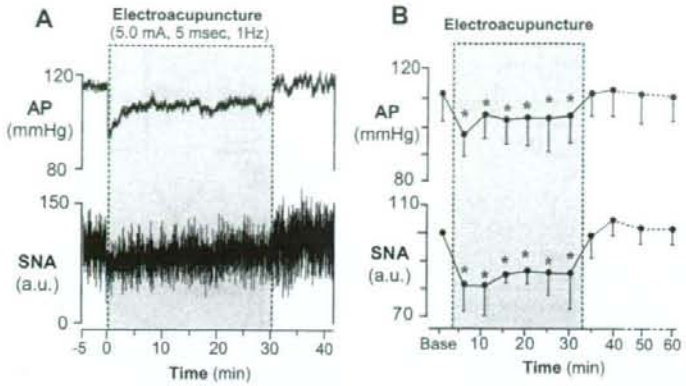

Fig. 6. Typical time series of AP and SNA during 30 min of 1-Hz electroacupuncture (St 36–39; *A*) and the averaged (n = 6) AP and SNA (*B*) in *protocol 3*. Data include periods of baseline (5 min), electroacupuncture (30 min), and recovery (30 min). Each data point represents averaged values over 5 min during baseline, electroacupuncture, and the first 10 min of recovery and those over 10 min during the last 20 min of recovery. *$P < 0.05$: significantly different from baseline after acupuncture insertion.

Another explanation for resetting in the neural arc may be circulatory endogenous opioids (e.g., β-endorphin and enkephalin), which are released from the adrenal gland and hypothalamus by prolonged (>30 min) electroacupuncture (20, 21). These endogenous opioids are known to modulate the arterial baroreflex (24, 29, 35). However, changes in endogenous opioids are unlikely to be the mechanism for reductions in SNA and AP by electroacupuncture in the present experimental settings because the inhibitory effects terminated immediately after cessation of electroacupuncture rather than lasting for several hours (42) (Fig. 1).

Previous studies suggest a central interaction between an electroacupuncture-evoked somatosympathetic reflex and the arterial baroreflex. Baroreceptor afferent inputs inhibit neural activities in the rostral ventrolateral medulla (rVLM) (6, 33). Tjen-A-Looi et al. (36) showed that electroacupuncture inhibited rVLM neural activities, suggesting that the electroacupuncture-evoked somatosympathetic reflex and arterial baroreflex share common central pathways. In addition, 2-Hz electroacupuncture inhibits SNA through the excitation of β-endorphinergic and GABAergic neurons to rVLM (12, 13).

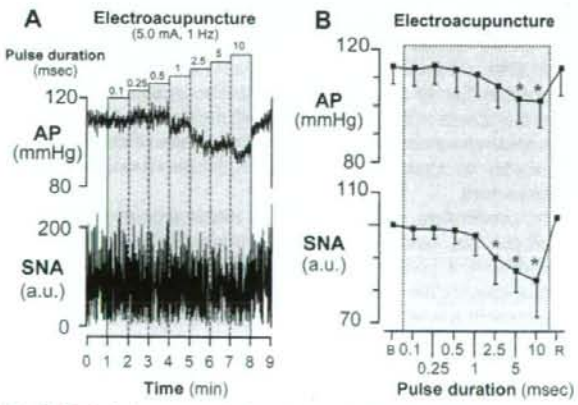

Fig. 7. Typical time series of AP and SNA during 1-Hz electroacupuncture with increasing the pulse duration (*A*) and the averaged (n = 6) AP and SNA (*B*) in *protocol 4*. Data include periods of baseline (B, 1 min), electroacupuncture (7 min), and recovery (R, 1 min). Each data point represents average values over 1 min. *$P < 0.05$; significantly different from baseline after acupuncture insertion.

Central interaction in the brain stem may be involved in the resetting of the arterial baroreflex neural arc induced by electroacupuncture.

Characteristics of Zusanli-Xiajuxu Electroacupuncture Used in the Present Study

The Zusanli electroacupuncture used in this study has some unique characteristics. First, our results showed that baseline AP and SNA were decreased significantly by electroacupuncture, in contrast to previous studies that found no significant reduction in baseline AP and SNA during Zusanli electroacupuncture in rats (0.5-ms duration, 1–2 mA, 2 Hz) (18) and nonelectrical acupuncture in normotensive humans (right large intestine 4, right liver 3, and left spleen 6) (22). Second, our result showed that AP and SNA were reduced as soon as electroacupuncture was started, in contrast to previous reports that the effect of Zusanli electroacupuncture did not even begin to manifest for the first 10–15 min in rats (0.5-ms duration, 1–2 mA, 2 Hz) (18) and cats (0.5-ms duration, 0.4–0.6 mA, 2–4 Hz) (37). These discrepancies may be related to the differences in acupoints and stimulation conditions (pulse duration, current, and frequency). In particular, the pulse duration used in our study (5 ms) was approximately 10–50 times longer than that used in previous studies. Indeed, the data obtained from *protocol 4* show that increasing the pulse duration augments the reduction in AP and SNA during electroacupuncture; pulse durations shorter than 2.5 ms did not change AP and SNA, whereas durations of 2.5 ms and above decreased both parameters immediately after the electroacupuncture was started (Fig. 7). In addition, our data suggest that stimulation duration (<2.5 ms) does not affect arterial baroreflex, consistent with our preliminary data that baroreflex neural, peripheral, and total arcs remained unchanged during electroacupuncture with pulse durations <2.5 ms (unpublished data). These observations may indicate that the effect of electroacupuncture on arterial baroreflex is linked to the stimulation pulse duration.

The third characteristic is that the inhibitory effects of electroacupuncture on AP and SNA disappeared immediately after the cessation of electroacupuncture. In contrast, some studies showed that the inhibitory effects of electroacupuncture on AP lasted for 10–60 min after the cessation (18). The characteristics in this study may not be explained by the length of electroacupuncture because AP and SNA recovered to the

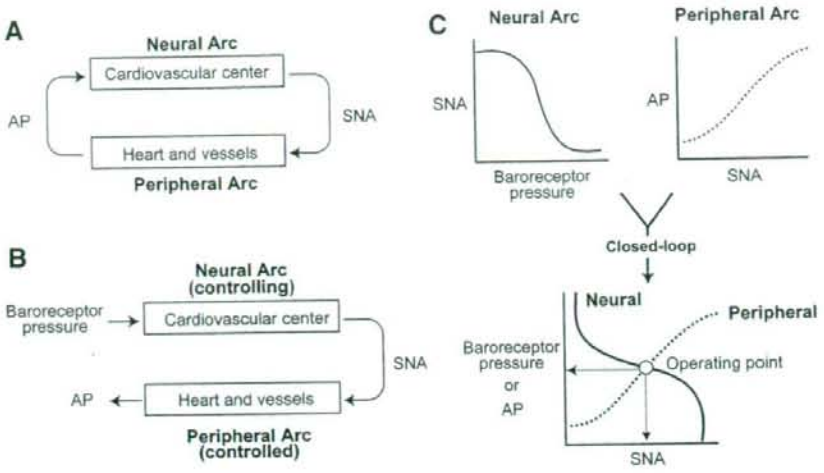

Fig. 8. Arterial baroreflex system in closed-loop (*A*) and open-loop (*B*) conditions. In open-loop conditions, the relationships between baroreceptor pressure and SNA (the neural arc) and between SNA and AP (the peripheral arc) can be quantitatively measured. Intersection of the neural and peripheral arcs corresponds to the operating point of AP and SNA under closed-loop conditions of feedback (*C*).

prestimulation baseline levels immediately after the cessation in both short-duration (8 min, Fig. 1) and longer-duration electroacupuncture (30 min, Fig. 6) protocols. The rapid disappearance of effects suggests that the AP and SNA reductions seen in the present study may not be elicited by the opioid mechanism, although clinical experiments with longer-duration electroacupuncture have demonstrated long-lasting effects on the cardiovascular system, which are attributed to opioid substances (2, 12, 15, 37, 42).

The reductions in AP and SNA during Zusanli electroacupuncture seen in the present study may not be just a nonspecific response to acupunctures. Our data from *protocol 2* (Fig. 5) showed that nonelectrical acupuncture at Zusanli (sham acupuncture) did not decrease AP and SNA, suggesting that the AP and SNA reductions during Zusanli electroacupuncture are not simply the results from insertion of acupuncture needles. Furthermore, acupuncture at Guangming-Xuanzhong (control acupuncture, control electroacupuncture) did not change AP and SNA regardless of electrical stimulation (Fig. 5). This result suggests the importance of acupoint specificity and is consistent with an earlier study showing point-specific differences in cardiovascular inhibitory responses (Jiangshi-Neiguan or Shousanli-Quchi acupoints vs. Pianli-Wenlui or Zusanli-Shangjuxu acupoints) (37). These observations may support the concept that Zusanli acupuncture changes cardiovascular variables in experimental animal models (4, 25, 28) and confers beneficial effects on cardiovascular diseases (5, 30, 34), whereas Guangming-Xuanzhong acupuncture does not affect cardiovascular variables (18).

Limitations

There are several limitations to this study. First, as anesthesia affects the autonomic nervous system, the results might have been different without anesthesia. Second, our isolation of the carotid sinus regions may stimulate carotid chemoreceptors. However, in determining baroreflex function, this factor was present in trials with and without electroacupuncture. Therefore, we believe that this factor may not affect our conclusion of baroreflex resetting during electroacupuncture.

Third, acupuncture was inserted at a point corresponding to the Zusanli acupoint in humans. When acupuncture is properly inserted at the acupoint, the patient feels heaviness or soreness. Such sensory information is not available in an anesthetized animal. Because electroacupuncture (as distinct from acupuncture with no electrical stimulation) stimulates not only the inserted point but also the surrounding area, it has been used as a convenient way of stimulating acupoints in patients and in experimental animals. Thus, even if we failed to insert the needle at the precise acupoint, we believe that Zusanli could be stimulated electrically.

Fourth, although we determined the effects of electroacupuncture at Zusanli acupoints on cardiovascular and baroreflex systems, there are other important acupoints that are able to influence these systems. In particular, Neiguan electroacupuncture is actually known to decrease sympathetic premotor neuron activity for a longer period than Zusanli electroacupuncture (36, 37). Further studies are necessary to determine the effect of Neiguan electroacupuncture on the arterial baroreflex.

Last, we evaluated the effects of Zusanli electroacupuncture on the baroreflex function for a short acupuncture duration of only 8 min. Because electroacupuncture is typically practiced for longer periods of time, our results have limited applicability. However, the electroacupuncture we used decreased AP and SNA immediately after application, showing that the procedure has acute effect on the cardiovascular system. That was the reason why we focused on the effect of short duration electroacupuncture on the baroreflex system. Future study is necessary to examine the effects of longer-duration electroacupuncture.

In conclusion, 1 Hz, short-term electroacupuncture of Zusanli reset the baroreflex neural arc toward lower SNA but did not affect the peripheral arc. The closed-loop operating point determined by the intersection of the neural and peripheral arcs was moved toward lower SNA and AP by electroacupuncture.

APPENDIX

Theoretical Considerations: Coupling of Neural and Peripheral Arcs

Changes in AP are immediately sensed by arterial baroreceptors, which alter efferent SNA via the cardiovascular center of baroreflex (Fig. 8*A*). Efferent SNA in turn governs heart rate and the mechanical

properties of the heart and vessels, which themselves exert a direct influence over AP. This negative-feedback loop makes it difficult to analyze the behavior of the arterial baroreflex. To overcome this problem, we opened the negative-feedback loop and divided the system into controlling and controlled elements (31). We defined the controlling element as the neural arc and the controlled element as the peripheral arc (Fig. 8*B*). In the neural arc, the input is the pressure sensed by the arterial baroreceptors and the output is SNA. In the peripheral arc, the input is SNA and the output is AP (Fig. 8*C*). Because pressure sensed by the arterial baroreceptor is equilibrated with AP under physiological conditions, we superimposed the functions of the two arcs and determined the operating point of the system from the intersection of the two arcs. The operating point is defined as the AP and SNA under closed-loop conditions of the feedback system. The validity of this framework has been examined in previous studies (10, 31). Using the baroreflex equilibrium diagram, we aimed to quantify the effects of electroacupuncture on the arterial baroreflex.

GRANTS

This study was supported by Health and Labor Sciences Research Grant for Research on Advanced Medical Technology from the Ministry of Health, Labour, and Welfare of Japan (H14-Nano-002), by a Grant-in-Aid for Scientific Research (A) (15200040) from the Japan Society for the Promotion of Science, the Program for Promotion of Fundamental Studies in Health Science from the Pharmaceutical and Medical Devices Agency of Japan, and by the "Ground-based Research Announcement for Space Utilization" project promoted by Japan Space Forum. This study was also supported by Industrial Technology Research Grant Program in 03A47075 from New Energy and Industrial Technology Development Organization (NEDO) of Japan.

REFERENCES

1. **Brickman AL, Calaresu FR, and Mogenson GJ.** Bradycardia during stimulation of the septum and somatic afferents in the rabbit. *Am J Physiol Regul Integr Comp Physiol* 236: R225–R230, 1979.
2. **Chao DM, Shen LL, Tjen-A-Looi S, Pitsillides KF, Li P, and Longhurst JC.** Naloxone reverses inhibitory effect of electroacupuncture on sympathetic cardiovascular reflex responses. *Am J Physiol Heart Circ Physiol* 276: H2127–H2134, 1999.
3. **Chen S and Ma SX.** Nitric oxide in the gracile nucleus mediates depressor response to acupuncture (ST36). *J Neurophysiol* 90: 780–785, 2003.
4. **Chiu DTJ and Cheng KK.** A study of the mechanism of the hypotensive effect of acupuncture in the rat. *Am J Chin Med* 2: 413–419, 1974.
5. **Chiu YJ, Chi A, and Reid IA.** Cardiovascular and endocrine effects of acupuncture in hypertensive patients. *Clin Exp Hypertens* 19: 1047–1063, 1997.
6. **Dampney RA, Horiuchi J, Tagawa T, Fontes MA, Potts PD, and Polson JW.** Medullary and supramedullary mechanisms regulating sympathetic vasomotor tone. *Acta Physiol Scand* 177: 209–218, 2003.
7. **Johansson B.** Studies on cardiovascular responses induced by electrical stimulation of afferent somatic nerves. A preliminary report. *Med Exp Int J Exp Med* 5: 447–453, 1961.
8. **Johansson B.** Circulatory responses to stimulation of somatic afferents with special reference to depressor effects from muscle nerves. *Acta Physiol Scand Suppl* 198: 1–91, 1962.
9. **Johansson B, Lundgren O, and Mellander S.** Reflex influence of "somatic pressor and depressor afferents" on resistance and capacitance vessels and on transcapillary fluid exchange. *Acta Physiol Scand* 62: 280–286, 1964.
10. **Kawada T, Shishido T, Inagaki M, Zheng C, Yanagiya Y, Uemura K, Sugimachi M, and Sunagawa K.** Estimation of baroreflex gain using a baroreflex equilibrium diagram. *Jpn J Physiol* 52: 21–29, 2002.
11. **Kent BB, Drane JW, Blumenstein B, and Manning JW.** A mathematical model to assess changes in the baroreceptor reflex. *Cardiology* 57: 295–310, 1972.
12. **Ku YH and Chang YZ.** β-Endorphin- and GABA-mediated depressor effect of specific electroacupuncture surpasses pressor response of emotional circuit. *Peptides* 22: 1465–1470, 2001.
13. **Ku YH and Zou CJ.** Beta-endorphinergic neurons in nucleus arcuatus and nucleus tractus solitarii mediated depressor-bradycardia effect of "Tinggong" 2-Hz electroacupuncture. *Acupunct Electrother Res* 18: 175–184, 1993.
14. **Legramante JM, Raimondi G, Adreani CM, Sacco S, Iellamo F, Peruzzi G, and Kaufman MP.** Group III muscle afferents evoke reflex depressor responses to repetitive muscle contractions in rabbits. *Am J Physiol Heart Circ Physiol* 278: H871–H877, 2000.
15. **Li L, Yin-Xiang C, Hong X, Peng L, and Da-Nian Z.** Nitric oxide in vPAG mediates the depressor response to acupuncture in stress-induced hypertensive rats. *Acupunct Electrother Res* 26: 165–170, 2001.
16. **Li P.** The effect of acupuncture on blood pressure: the interrelation of sympathetic activity and endogenous opeoid peptides. *Acupunct Electrother Res* 8: 45–56, 1983.
17. **Li P, Pitsillides KF, Rendig SV, Pan HL, and Longhurst JC.** Reversal of reflex-induced myocardial ischemia by median nerve stimulation: a feline model of electroacupuncture. *Circulation* 97: 1186–1194, 1998.
18. **Li P, Rowshan K, Crisostomo M, Tjen-A-Looi SC, and Longhurst JC.** Effect of electroacupuncture on pressor reflex during gastric distension. *Am J Physiol Regul Integr Comp Physiol* 283: R1335–R1345, 2002.
19. **Li P, Tjen-A-Looi S, and Longhurst JC.** Rostral ventrolateral medullary opioid receptor subtypes in the inhibitory effect of electroacupuncture on reflex autonomic response in cats. *Auton Neurosci* 89: 38–47, 2001.
20. **Lin JG, Chang SL, and Cheng JT.** Release of beta-endorphin from adrenal gland to lower plasma glucose by the electroacupuncture at Zhongwan acupoint in rats. *Neurosci Lett* 326: 17–20, 2002.
21. **Lin JG, Lo MW, Wen YR, Hsieh CL, Tsai SK, and Sun WZ.** The effect of high and low frequency electroacupuncture in pain after lower abdominal surgery. *Pain* 99: 509–514, 2002.
22. **Middlekauff HR, Yu JL, and Hui K.** Acupuncture effects on reflex responses to mental stress in humans. *Am J Physiol Regul Integr Comp Physiol* 280: R1462–R1468, 2001.
23. **Mohrman DE and Heller LJ.** *Cardiovascular Physiology* (4th ed.). New York: McGraw-Hill, 1997, p. 158–230.
24. **Moore PG, Quail AW, Cottee DB, McIlveen SA, and White SW.** Effect of fentanyl on baroreflex control of circumflex coronary conductance. *Clin Exp Pharmacol Physiol* 27: 1028–1033, 2000.
25. **Mori H, Uchida S, Ohsawa H, Noguchi E, Kimura T, and Nishijo K.** Electro-acupuncture stimulation to a hindpaw and a hind leg produces different reflex responses in sympathoadrenal medullary function in anesthetized rats. *J Auton Nerv Syst* 79: 93–98, 2000.
26. **Nishijo K, Mori H, Yosikawa K, and Yazawa K.** Decreased heart rate by acupuncture stimulation in humans via facilitation of cardiac vagal activity and suppression of cardiac sympathetic nerve. *Neurosci Lett* 227: 165–168, 1997.
27. **Ohsawa H, Okada K, Nishijo K, and Sato Y.** Neural mechanism of depressor responses of arterial pressure elicited by acupuncture-like stimulation to a hindlimb in anesthetized rats. *J Auton Nerv Syst* 51: 27–35, 1995.
28. **Ohsawa H, Yamaguchi S, Ishimaru H, Shimura M, and Sato Y.** Neural mechanism of pupillary dilation elicited by electro-acupuncture stimulation in anesthetized rats. *J Auton Nerv Syst* 64: 101–106, 1997.
29. **Petty MA and Reid JL.** The effect of opiates on arterial baroreceptor reflex function in the rabbit. *Naunyn Schmiedebergs Arch Pharmacol* 319: 206–211, 1982.
30. **Richter A, Herlitz J, and Hjalmarson A.** Effect of acupuncture in patients with angina pectoris. *Eur Heart J* 12: 175–178, 1991.
31. **Sato T, Kawada T, Inagaki M, Shishido T, Takaki H, Sugimachi M, and Sunagawa K.** New analytic framework for understanding sympathetic baroreflex control of arterial pressure. *Am J Physiol Heart Circ Physiol* 276: H2251–H2261, 1999.
32. **Si QM, Wu GC, and Cao XD.** Effects of electroacupuncture on acute cerebral infarction. *Acupunct Electrother Res* 23: 117–124, 1998.
33. **Sved AF, Ito S, and Madden CJ.** Baroreflex dependent and independent roles of the caudal ventrolateral medulla in cardiovascular regulation. *Brain Res Bull* 51: 129–133, 2000.
34. **Tam KC and Yiu HH.** The effect of acupuncture on essential hypertension. *Am J Chin Med* 3: 369–375, 1975.
35. **Taneyama C, Goto H, Kohno N, Benson KT, Sasao J, and Arakawa K.** Effects of fentanyl, diazepam, and the combination of both on arterial baroreflex and sympathetic nerve activity in intact and baro-denervated dogs. *Anesth Analg* 77: 44–48, 1993.
36. **Tjen-A-Looi SC, Li P, and Longhurst JC.** Prolonged inhibition of rostral ventral lateral medullary premotor sympathetic neurons by electroacupuncture in cats. *Auton Neurosci* 106: 119–131, 2003.

37. **Tjen-A-Looi SC, Peng L, and Longhurst JC.** Medullary substrate and differential cardiovascular responses during stimulation of specific acupoints. *Am J Physiol Regul Integr Comp Physiol* 287: R852–R862, 2004.
38. **Wang JD, Kuo TB, and Yang CC.** An alternative method to enhance vagal activities and suppress sympathetic activities in humans. *Auton Neurosci* 100: 90–95, 2002.
39. **Wong AM, Leong CP, Su TY, Yu SW, Tsai WC, and Chen CP.** Clinical trial of acupuncture for patients with spinal cord injuries. *Am J Phys Med Rehabil* 82: 21–27, 2003.
40. **Wong AM, Su TY, Tang FT, Cheng PT, and Liaw MY.** Clinical trial of electrical acupuncture on hemiplegic stroke patients. *Am J Phys Med Rehabil* 78: 117–122, 1999.
41. **Yamamoto K, Kawada T, Kamiya A, Takaki H, Miyamoto T, Sugimachi M, and Sunagawa K.** Muscle mechanoreflex induces the pressor response by resetting the arterial baroreflex neural arc. *Am J Physiol Heart Circ Physiol* 286: H1382–H1388, 2004.
42. **Yao T.** Acupuncture and somatic nerve stimulation: mechanism underlying effects on cardiovascular and renal activities. *Scand J Rehabil Med Suppl* 29: 7–18, 1993.

J Appl Physiol 100: 1278–1286, 2006.
First published December 22, 2005; doi:10.1152/japplphysiol.01206.2005.

TRANSLATIONAL PHYSIOLOGY

Automated drug delivery system to control systemic arterial pressure, cardiac output, and left heart filling pressure in acute decompensated heart failure

Kazunori Uemura,[1] Atsunori Kamiya,[1] Ichiro Hidaka,[1] Toru Kawada,[1] Shuji Shimizu,[1] Toshiaki Shishido,[1] Makoto Yoshizawa,[2] Masaru Sugimachi,[1] and Kenji Sunagawa[3]

[1]*Department of Cardiovascular Dynamics, National Cardiovascular Center Research Institute, Suita;* [2]*Research Division on Advanced Information Technology, Information Synergy Center, Tohoku University, Sendai;* [3]*Department of Cardiovascular Medicine, Kyushu University Graduate School of Medical Science, Fukuoka, Japan*

Submitted 22 September 2005; accepted in final form 17 December 2005

Uemura, Kazunori, Atsunori Kamiya, Ichiro Hidaka, Toru Kawada, Shuji Shimizu, Toshiaki Shishido, Makoto Yoshizawa, Masaru Sugimachi, and Kenji Sunagawa. Automated drug delivery system to control systemic arterial pressure, cardiac output, and left heart filling pressure in acute decompensated heart failure. *J Appl Physiol* 100: 1278–1286, 2006. First published December 22, 2005; doi:10.1152/japplphysiol.01206.2005.—Pharmacological support with inotropes and vasodilators to control decompensated hemodynamics requires strict monitoring of patient condition and frequent adjustments of drug infusion rates, which is difficult and time-consuming, especially in hemodynamically unstable patients. To overcome this difficulty, we have developed a novel automated drug delivery system for simultaneous control of systemic arterial pressure (AP), cardiac output (CO), and left atrial pressure (Pla). Previous systems attempted to directly control AP and CO by estimating their responses to drug infusions. This approach is inapplicable because of the difficulties to estimate simultaneous AP, CO, and Pla responses to the infusion of multiple drugs. The circulatory equilibrium framework developed previously (Uemura K, Sugimachi M, Kawada T, Kamiya A, Jin Y, Kashihara K, and Sunagawa K. *Am J Physiol Heart Circ Physiol* 286: H2376–H2385, 2004) indicates that AP, CO, and Pla are determined by an equilibrium of the pumping ability of the left heart (S_L), stressed blood volume (V), and systemic arterial resistance (R). Our system directly controls S_L with dobutamine, V with dextran/furosemide, and R with nitroprusside, thereby controlling the three variables. We evaluated the efficacy of our system in 12 anesthetized dogs with acute decompensated heart failure. Once activated, the system restored S_L, V, and R within 30 min, resulting in the restoration of normal AP, CO, and Pla. Steady-state deviations from target values were small for AP [4.4 mmHg (SD 2.6)], CO [5.4 ml·min^{-1}·kg^{-1} (SD 2.4)] and Pla [0.8 mmHg (SD 0.6)]. In conclusion, by directly controlling the mechanical determinants of circulation, our system has enabled simultaneous control of AP, CO, and Pla with good accuracy and stability.

computers; negative feedback; circulatory equilibrium

IN THE MANAGEMENT OF PATIENTS with acute decompensated heart failure after myocardial infarction or after cardiac surgical procedures, cardiovascular agents such as inotropes and/or vasodilators are commonly used to control systemic arterial pressure (AP), cardiac output (CO), and left heart filling pressure (2, 13, 20). Because responses to these agents vary between patients and within patient over time, strict monitoring of patient condition and frequent adjustments of drug infusion rates are usually required. This is a difficult and time-consuming process, especially in hemodynamically unstable patients. Several closed-loop systems to automate drug infusion have been developed to facilitate this process (10, 11, 18, 26, 27). Closed-loop control of AP with vasodilators was more precise and stable than manual controls (10, 11). Chitwood et al. (10) demonstrated that, compared with manual control, closed-loop control of postoperative hypertension significantly improves patient outcome by reducing the transfusion requirement and postoperative blood loss. Although closed-loop control of hemodynamics has been suggested to be useful in clinical settings, no closed-loop system so far developed is capable of controlling the overall hemodynamics; i.e., controlling AP, CO, and left heart filling pressure simultaneously (18). This is because all previous systems attempted to directly control the hemodynamic variable by estimating response of the variable to drug infusion (10, 11, 18, 26, 27). Although such an approach worked well in controlling a single variable, it cannot be applied to control of the three variables, because it is difficult to simultaneously estimate their responses to the infusions of multiple drugs.

In this study, we developed a new automated drug delivery system that is capable of controlling AP, CO, and left atrial pressure (Pla). We modeled the entire cardiovascular system by extending Guyton's framework of circulatory equilibrium (16, 17, 24, 25). As shown in Fig. 1, the extended framework consists of an integrated cardiac output curve characterizing the pumping ability of the left and the right heart and a venous return surface characterizing the venous return property of the systemic and pulmonary circulation (24, 25). The intersection point of the integrated CO curve and the venous return surface predicts the equilibrium point of CO, Pla, and right atrial pressure (Pra) (Fig. 1) (24, 25). Once CO, Pla, and Pra are predicted from the intersection point, systemic arterial resistance determines AP. On the basis of this framework, instead of directly controlling AP, CO, and Pla, our system controls the integrated CO curve with dobutamine (Dob), the venous return surface with 10% dextran 40 (Dex) and furosemide (Fur), and systemic arterial resistance with sodium nitroprusside (SNP), thereby controlling the three hemodynamic variables.

Address for reprint requests and other correspondence: K. Uemura, Dept. of Cardiovascular Dynamics, National Cardiovascular Center Research Institute, 5-7-1 Fujishirodai, Suita 565-8565, Japan (e-mail: kuemura@ri.ncvc.go.jp).

The costs of publication of this article were defrayed in part by the payment of page charges. The article must therefore be hereby marked "*advertisement*" in accordance with 18 U.S.C. Section 1734 solely to indicate this fact.

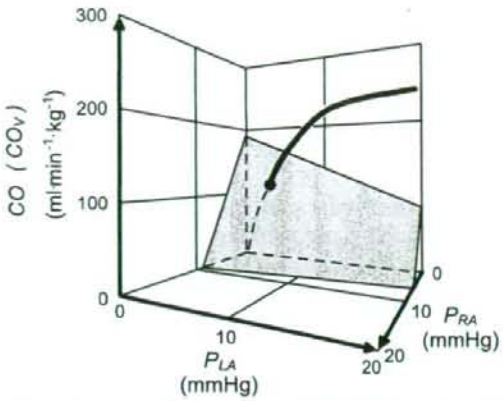

Fig. 1. Diagram of circulatory equilibrium for cardiac output (CO), venous return (CO_V), left atrial pressure (Pla), and right atrial pressure (Pra). The equilibrium CO, Pla, and Pra are obtained as the intersection point of the venous return surface and integrated cardiac output curve. [Modified from Uemura et al. (Ref 25).]

The purpose of this study was, therefore, to develop and validate the new automated drug delivery system. We evaluated the efficacy of our system in a canine model of acute ischemic heart failure. Our results indicated that this novel automated drug delivery system was able to control AP, CO, and Pla simultaneously with reasonably good accuracy and stability.

METHODS

Cardiac Output Curve, Venous Return Surface, and Arterial Resistance

On the basis of previous studies, we parameterized the integrated CO curve by the pumping ability of the left heart (S_L), the venous return surface by total stressed blood volume (V), and the systemic arterial resistance by R (see APPENDIX A) (24, 25). Our system aims to control these cardiovascular parameters to achieve target AP (AP*), target CO (CO*), and target Pla (Pla*).

Automated Drug Delivery System

Figure 2*A* illustrates a block diagram of the automated drug delivery system, using a negative feedback mechanism.

Target values of S_L (S_L*), V (V*), and R (R*) are determined according to the AP*, CO*, and Pla* (see APPENDIX B). The subject's S_L, V, and R are calculated from the measured AP, CO, Pla, and Pra (Fig. 2*A*). S_L, V, and R are compared with S_L*, V*, and R*, respectively.

To minimize the difference between S_L* and S_L ($\Delta S_L = S_L^* - S_L$) and the difference between R* and R ($\Delta R = R^* - R$), proportional-integral (PI) feedback controllers adjusts infusion rates of Dob and SNP, respectively (Fig. 2*A*). In the PI controller (Fig. 2*B*), ΔS_L (or ΔR) and the difference integrated with an integral gain (K_i) are summed and scaled by a proportional gain (K_p) to give the infusion rate of Dob (or SNP). We determined values of K_i and K_p on the

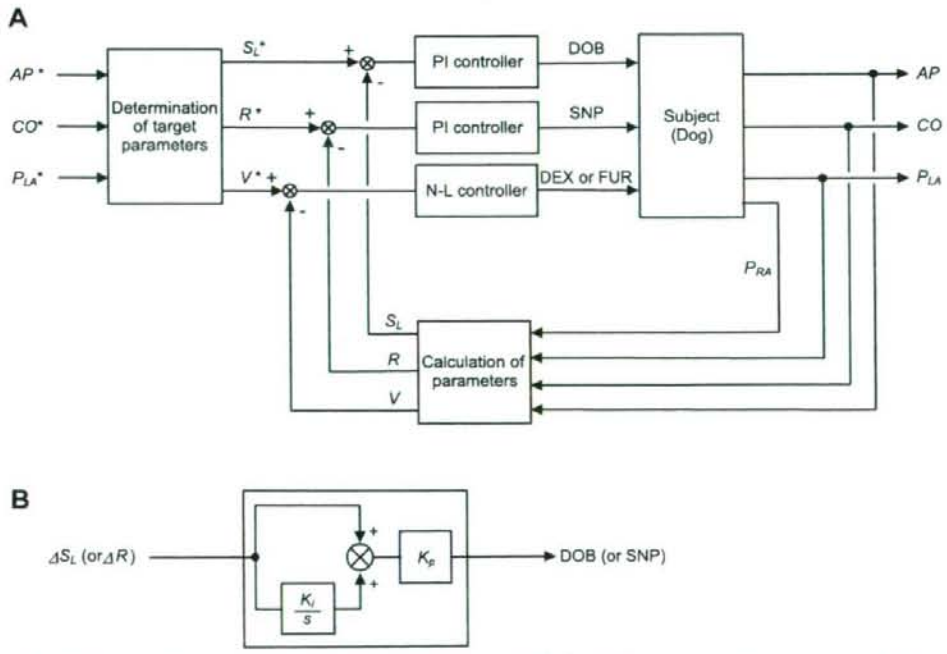

Fig. 2. *A*: block diagram of an automated drug delivery system for simultaneous control of systemic arterial pressure (AP), CO, and Pla. AP*, CO* and Pla* represent target AP, target CO, and target Pla, respectively. From these target variables, target values of pumping ability of the left heart (S_L*), stressed blood volume (V*), and systemic arterial resistance (R*) are determined. Subject's S_L, V, and R are calculated from measured AP, CO, Pla, and Pra. Proportional-integral (PI) controllers adjust infusion rate of dobutamine (Dob) and sodium nitroprusside (SNP) to minimize the difference between S_L and S_L* (ΔS_L), and the difference between R and R* (ΔR), respectively. Nonlinear (N-L) controller adjusts infusion of 10% dextran 40 (Dex) or injection of furosemide (Fur) so that the difference between V and V* is minimized. *B*: block diagram of the PI controller. K_i and K_p represent the integral and proportional gain constants, respectively; s is a Laplace operator.

basis of open-loop response of S_L (or R) to the infusion of Dob (or SNP) (4, 9).

To minimize the difference between V* and V ($\Delta V = V^*-V$), a nonlinear (NL) feedback controller (Fig. 2*A*) adjusts the infusion of Dex or injection of Fur on the basis of the following "if-then" rules:

Rule 1: If $\Delta V \geq X_1$ ml/kg then infuse Dex (Y_1, ml/min)

Rule 2: If $\Delta V \leq X_2$ ml/kg then inject Fur (Y_2, mg)

We determined values of X_1, Y_1, X_2, and Y_2 on the basis of the open-loop response of V to the infusion of Dex and Fur.

These adjustment processes are repeated in parallel and continued until the differences disappear.

Preparation

We used 35 adult mongrel dogs in this study [both sexes, body weight 25 kg (SD 4)]. Care of the animals was in strict accordance with the guiding principles of the Physiological Society of Japan. All protocols were approved by the Animal Subjects Committee of the National Cardiovascular Center. Anesthesia was induced with pentobarbital sodium (25 mg/kg). Animals were intubated endotracheally. Isoflurane (1.0%) was inhaled continuously to maintain an appropriate level of anesthesia during the experiment. A catheter (8-Fr) was placed in the right femoral artery, which was connected to a pressure transducer (DX-200, Nihon Kohden, Tokyo, Japan) to measure AP. After a median sternotomy, a small pericardial incision was made at the level of the aortic root. Through the incision, an ultrasonic flow meter (20A594, Transonics, Ithaca, NY) was placed around the ascending aorta to measure CO. Fluid-filled catheters were placed in the left and right atria to measure Pla and Pra, respectively. They were connected to pressure transducers (DX-200, Nihon Kohden). The junction between the vena cavae and the right atrium was taken as the reference point for zero pressure. The undamped natural frequency and the damping ratio of the fluid filled catheters for the pressure measurements were 21 Hz and 0.22, respectively. A urinary catheter was inserted to measure urine volume.

A catheter (6-Fr) was placed in the right femoral vein. A roller pump (Minipuls 3, Gilson, Middleton, WI) was attached to the venous line to infuse Dex. A double-lumen catheter was also introduced into the right femoral vein for administration of Dob and SNP. Infusion pumps (CFV-3200, Nihon Kohden) were used for Dob and SNP infusion. The infusion rates of Dex, Dob, and SNP were controlled with a personal computer (MA20V, NEC, Tokyo, Japan) through a 12-bit digital-to-analog converter (DA12-8PCI, Contec, Osaka, Japan). A catheter (6-Fr) was placed in the right external jugular vein, from which Fur was injected after a command signal from the computer.

Experimental Protocols

We induced left ventricular failure (LVF) in all the animals by embolizing the left circumflex coronary artery with glass microspheres (90 μm in diameter) (24, 25). We adjusted the amount of injected microspheres to increase Pla to more than 18 mmHg or decrease CO to less than 70 $ml \cdot min^{-1} \cdot kg^{-1}$. When ventricular tachycardia or frequent premature ventricular contractions were noted, lidocaine (1 mg/min) was infused to suppress the arrhythmia.

Response of cardiovascular parameters to drug infusion. Under open-loop conditions, we examined the response of cardiovascular parameters to drug infusions in 21 dogs with LVF. In 10 dogs, we infused Dob in a stepwise manner at 6 $\mu g \cdot kg^{-1} \cdot min^{-1}$ for 10 min to obtain a step response of S_L. In six dogs, we infused SNP at 2 $\mu g \cdot kg^{-1} \cdot min^{-1}$ for 10 min to obtain a step response of R. In five dogs, we infused Dex at 0.4 $ml \cdot min^{-1} \cdot kg^{-1}$ for 10 min to observe the response of V. In seven dogs, we injected Fur (20 mg, bolus iv) and observed the response of V and urine volume for 50 min.

Application of the automated drug delivery system. We applied the system to the other 14 dogs with LVF. We first defined AP* (90–105 mmHg), CO* (90–100 $ml \cdot min^{-1} \cdot kg^{-1}$), and Pla* (8–12 mmHg), which were fed into the system to determine S_L*, V*, and R* (see APPENDIX B). The controllers were then activated by closing the loops. In 12 dogs (*group 1*), we observed the performance of the system over 50–60 min. In two dogs (*group 2*), we observed the performance of the system over 100–150 min to evaluate stability of the closed-loop control over a longer periods of time.

With the use of the computer, analog signals of AP, CO, Pla, and Pra were digitized at 200 Hz with a 12-bit analog-to-digital converter [AD12-16U(PCI)E, Contec, Osaka, Japan] and stored on a hard disk for offline analysis. In the closed-loop control, the digitized signals were smoothed by a low-pass filter (time constant, 10 s) and were used as the system controlled variables. The infusion rates of Dob, SNP, and Dex were also stored. Urine volume after the injection of Fur was recorded.

Data Analysis

Evaluation of the response of cardiovascular parameters and design of the controller. We described the step response of S_L and R by a transfer function of a first-order model with a transport delay. In this model, change in S_L from baseline (δS_L) in response to Dob infusion can be expressed by the following formula:

$$\delta S_L(t) = \begin{cases} G \cdot \left[1 - \exp\left(-\dfrac{t-L}{T}\right)\right] & (t \geq L) \\ 0 & (t < L) \end{cases} \qquad (1)$$

where G is static gain $[ml \cdot min^{-1} \cdot kg^{-1} (\mu g \cdot kg^{-1} \cdot min^{-1})^{-1}]$, L is transport delay (s), and T is time constant (s). Change in R from baseline (δR) in response to the SNP infusion can be expressed similarly and is characterized by G $[mmHg \cdot min \cdot ml^{-1} \cdot kg (\mu g \cdot kg^{-1} \cdot min^{-1})^{-1}]$, L (s), and T (s). We estimated the parameters of the transfer function by approximating δS_L and δR to *Eq. 1* using the least square method. We averaged the parameters of the transfer function of S_L response for 10 animals and those of R response for 6 animals. The averaged parameters were used to determine the PI gain constants, K_I and K_P, in accordance with the method of Chien et al. (9). Their method provides PI constants that permit the regulated variable to respond rapidly without overshoot (4, 9).

We evaluated the change in V from baseline (δV) in response to the infusion of Dex and Fur. On the basis of δV, we determined the constants (X_1, Y_1, X_2, and Y_2) of the if-then rules.

Efficacy of the automated drug delivery system. We calculated the following indexes to evaluate the accuracy and stability of the control of AP, CO, and Pla by the new system: the time required for the hemodynamic variables to reach the acceptable ranges of the target values (±10 mmHg for AP, ±10 $ml \cdot min^{-1} \cdot kg^{-1}$ for CO, ±2 mmHg for Pla), and the standard deviations of the steady-state differences between AP and AP*, between CO and CO*, and between Pla and Pla*. Because steady states were reached within 30 min in all the variables in the present study, standard deviations were calculated from 30 min after the loop was closed.

Statistics

Group data are expressed as means (SD) unless otherwise stated. Student's paired *t*-test was used to compare hemodynamic data at baseline and after the coronary embolization. One-way ANOVA with Tukey's post hoc test was used to compare hemodynamic data before, during, and after the closed-loop control of hemodynamics. The level of statistical significance was defined as $P < 0.05$.

RESULTS

Hemodynamic data at baseline and after left circumflex coronary artery embolization are summarized in Table 1. Coronary embolization more than doubled Pla [from 7.5 (SD 1.9) to 19.4 (SD 6.2) mmHg] and halved CO [from 131.4 (SD

Table 1. *Hemodynamic data at baseline and after left circumflex coronary artery embolization*

	Baseline	Embolization
HR, beats/min	141.3 (19.5) [112.0–188.3]	146.2 (28.8) [81.4–197.9]
AP, mmHg	109.1 (18.7) [76.4–140.0]	90.9 (16.5) [66.9–135.6]*
CO, ml·min^{-1}·kg^{-1}	131.4 (40.9) [64.5–229.2]	66.8 (23.3) [30.3–121.7]*
Pla, mmHg	7.5 (1.9) [4.7–12.8]	19.4 (6.2) [7.9–34.5]*
Pra, mmHg	4.2 (1.2) [2.1–7.2]	6.0 (1.8) [3.5–9.9]*
S_L, ml·min^{-1}·kg^{-1}	54.3 (18.1) [25.2–105.9]	19.1 (7.6) [8.0–33.7]*
R, mmHg·min·ml^{-1}·kg	0.9 (0.4) [0.4–1.8]	1.4 (0.5) [0.7–2.6]*
V, ml/kg	31.0 (6.6) [21.7–45.2]	32.3 (4.9) [20.6–43.7]

Values are means (SD) (n = 35 in each group). Numbers in brackets are the ranges. HR, heart rate. AP, systemic arterial pressure; CO, cardiac output; Pla, left atrial pressure; Pra, right atrial pressure; S_L, pumping ability of the left heart; R, systemic arterial resistance; V, stressed blood volume. *$P < 0.01$ vs. baseline.

40.9) to 66.8 (SD 23.3) ml·min^{-1}·kg^{-1}]. This decreased S_L to about one-third of the baseline value, which indicates substantial downward shift of the left cardiac output curve. These changes are compatible with severe LVF.

Response of Cardiovascular Parameters to Drug Infusion

Figure 3 shows the open-loop responses of cardiovascular parameters to drug infusions. Figure 3, *A* and *B*, shows the averaged time course of δS_L during Dob infusion (n = 10) and that of δR during SNP infusion (n = 6), respectively. Dob infusion increased δS_L, and SNP infusion decreased δR exponentially. The results of the fit of δS_L and δR to *Eq. 1* are summarized in Table 2. The fact that the correlation coefficients were close to unity, with a small standard error of the estimate relative to the amount of δS_L and δR, suggested that the approximation of δS_L and δR to *Eq. 1* was reasonably accurate. On the basis of the averaged parameters of the transfer function (Table 2), we determined the PI gain constants for Dob infusion [K_i = 0.01 s^{-1}, K_p = 0.06 μg·kg^{-1}·min^{-1} (ml·min^{-1}·kg^{-1})$^{-1}$] and for SNP infusion [K_i = 0.007 s^{-1}, K_p = −1.37 μg·kg^{-1}·min^{-1} (mmHg·min·ml^{-1}·kg)$^{-1}$].

Figure 3*C* shows the averaged time course of δV in response to Dex infusion (n = 5). δV increased and plateaued [7.2 ml/kg (SD 2.2)] after the cessation of Dex infusion. δV at the plateau was greater than the total volume of Dex infused (4 ml/kg), suggesting transvascular fluid absorption by colloid osmotic pressure (3). Figure 3*D* shows the averaged time course of δV after a single intravenous injection of Fur (20 mg, n = 7). δV gradually decreased and reached a trough [−4.3 ml/kg (SD 3.5)] around 30 min after the Fur injection. Average urine volume was 180 ml (SD 94). On the basis of these responses, we determined the constants of the if-then rules as X_1 = 1 ml/kg, Y_1 = 10 ml/min, X_2 = −2 ml/kg, and Y_2 = 10 mg. To avoid oscillation between hypovole-

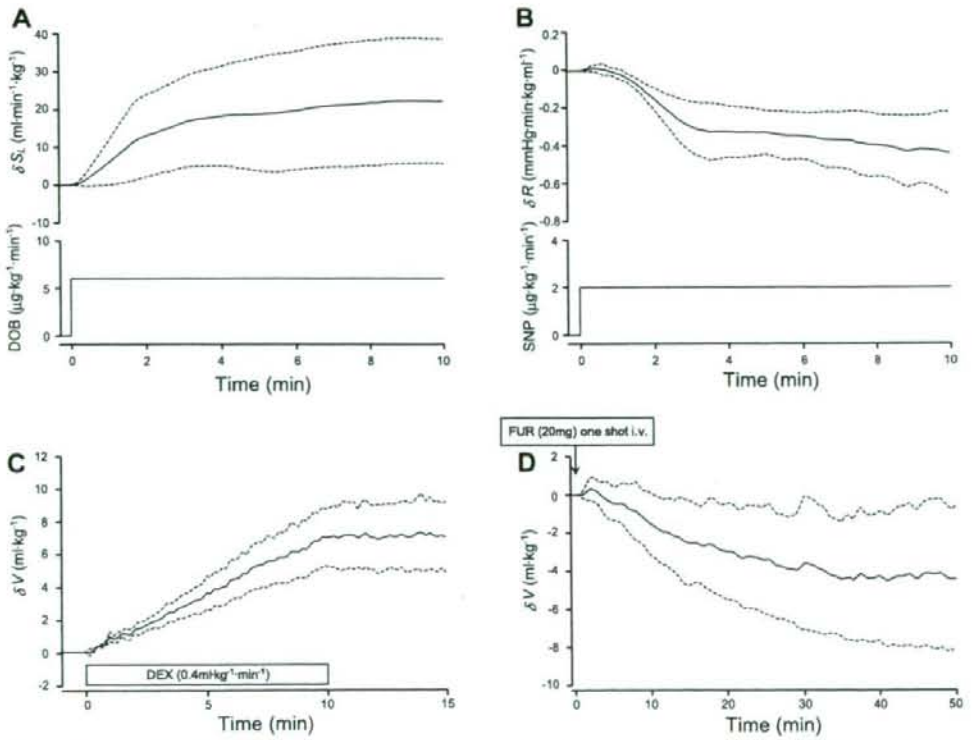

Fig. 3. Response of cardiovascular parameter to drug infusion. *A*: averaged response of S_L to stepwise Dob infusion (6 μg·kg^{-1}·min^{-1}) (n = 10). The ordinate indicates change in S_L from baseline (δS_L). *B*: averaged response of R to stepwise SNP infusion (2 μg·kg^{-1}·min^{-1}) (n = 6). The ordinate indicates change in R from baseline (δR). *C* and *D*: averaged response of V to Dex infusion (0.4 ml·min^{-1}·kg^{-1}) (*C*, n = 5) and to Fur (20 mg) injection (*D*, n = 7). The ordinates indicate change in V from baseline (δV). Data are expressed by mean (solid line) ± SD (broken line).

Table 2. *Parameters of step response of S_L and R*

	G	*L*	*T*	*r*	SEE
δS_L	3.6 (2.7)	63.5 (46.9)	79.0 (78.0)	0.91 (0.09)	2.0 (0.7)
δR	−0.21 (0.08)	69.8 (26.1)	117.1 (80.2)	0.93 (0.02)	0.06 (0.02)

Values are means (SD). δS_L, change in S_L from baseline; δR, change in R from baseline; *G*, static gain of δS_L [ml·min^{-1}·kg^{-1} (μg·kg^{-1}·min^{-1})$^{-1}$] and of δR [mmHg·min·ml^{-1}·kg (μg·kg^{-1}·min^{-1})$^{-1}$]; *L*, transport delay (s); *T*, time constant (s); *r*, correlation coefficient; SEE, standard error of the estimate of δS_L (ml·min^{-1}·kg^{-1}) and of δR (mmHg·min·ml^{-1}·kg).

rmia and hypervolemia (hence infusion of Dex and injection of Fur), we introduced a dead zone (-2 ml/kg $< \Delta V <$ 1 ml/kg) into the rules (4). We set continuous checking for *rule 1* and checking at 20-min intervals for *rule 2*.

With the controllers thus designed, we evaluated the performance of the automated system in the next protocol.

Performance of the Automated Drug Delivery System

Figure 4 shows the experimental trial in a representative case. The automated system was activated at 0 min. Figure 4*A* shows the time courses of the infusion rates of Dob and SNP and the accumulated volume of infused Dex. In this case, Fur was not injected. Figure 4*B* shows the time courses of S_L, R, and V. Infusion rates of Dob, SNP, and Dex were adjusted so that S_L, R, and V reached their respective target values. By controlling the cardiovascular parameters, the automated system controlled AP, CO, and Pla accurately and stably as demonstrated in Fig. 4*C*. AP, CO, and Pla reached their respective target levels within 30 min and remained at these levels.

Figure 5 summarizes the results obtained for 12 dogs (*group 1*), demonstrating the effectiveness of the performance of the automated system. Figure 5*A* shows averaged time courses of the infusion rates of Dob and SNP, and the accumulated volume of infused Dex. The average infusion rates of Dob and SNP were 4.7 μg·kg^{-1}·min^{-1} (SD 2.6) and 4.2 μg·kg^{-1}·min^{-1} (SD 1.8), respectively. The average volume of infused Dex was 2.4 ml/kg (SD 1.9). Fur was injected once in one animal and twice in another animal. In these two animals, V decreased by 3.8–10.2 ml/kg in response to the injection of Fur with a total urine volume of 250–300 ml. Figure 5*B* shows averaged time courses of difference between S_L and S_L* ($S_L - S_L$*), difference between R and R* (R − R*), and difference between V and V* (V − V*). Once the system was activated, these differences rapidly converged to the zero lines in all the animals. S_L was restored to subnormal conditions [33.0 ml·min^{-1}·kg^{-1} (SD 2.6)] irrespective of the magnitude of depression before the control [13.8 ml·min^{-1}·kg^{-1} (SD 3.5), from 9.4 to 20.5 ml·min^{-1}·kg^{-1}]. These resulted in accurate and stable control of AP, CO, and Pla (Fig. 5*C*). The ordinates of Fig. 5*C* indicate the difference between AP and AP* (AP − AP*), difference between CO and CO* (CO − CO*), and difference between Pla and Pla* (Pla − Pla*). These differences also converged to the zero lines rapidly. The average times for AP, CO, and Pla to reach the acceptable ranges were 5.2 min (SD 6.6), 6.8 min (SD 4.6), and 11.7 min (SD 9.8),

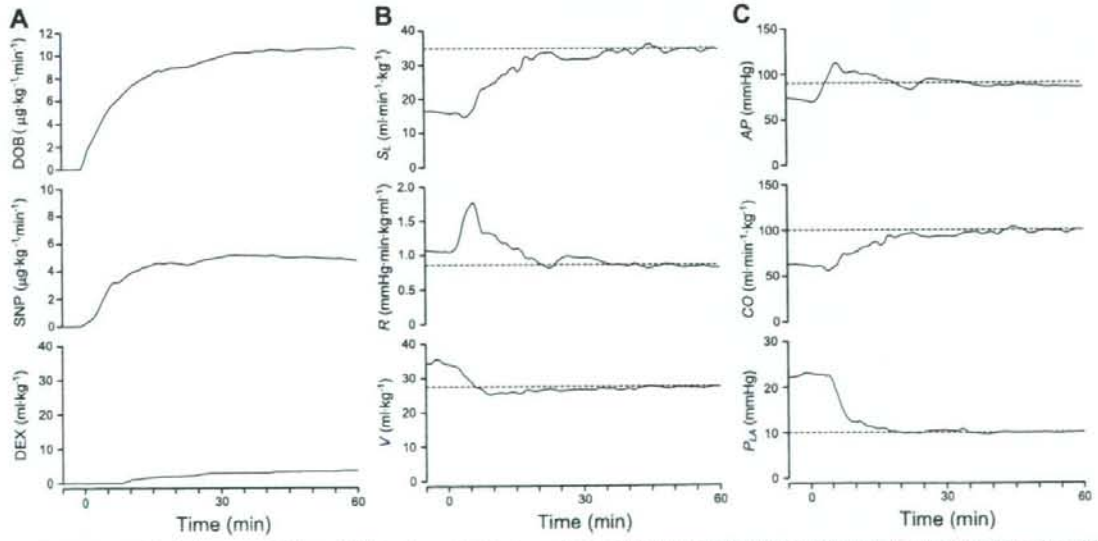

Fig. 4. Time courses of infusion rates of Dob and SNP, and cumulated volume of infused Dex (*A*), cardiovascular parameters (*B*), and hemodynamic variables (*C*) in 1 representative animal during closed-loop control of hemodynamics. Broken horizontal lines in *B* indicate target parameters (*top*, S_L*; *middle*, R*; *bottom*, V*). Broken horizontal lines in *C* indicate target hemodynamic variables (*top*, AP*; *middle*, CO*; *bottom*, Pla*). Drug infusion rates were adjusted so that the cardiovascular parameters reached the respective target values. As the parameters got closer to their targets, all 3 hemodynamic variables approached their respective target values.

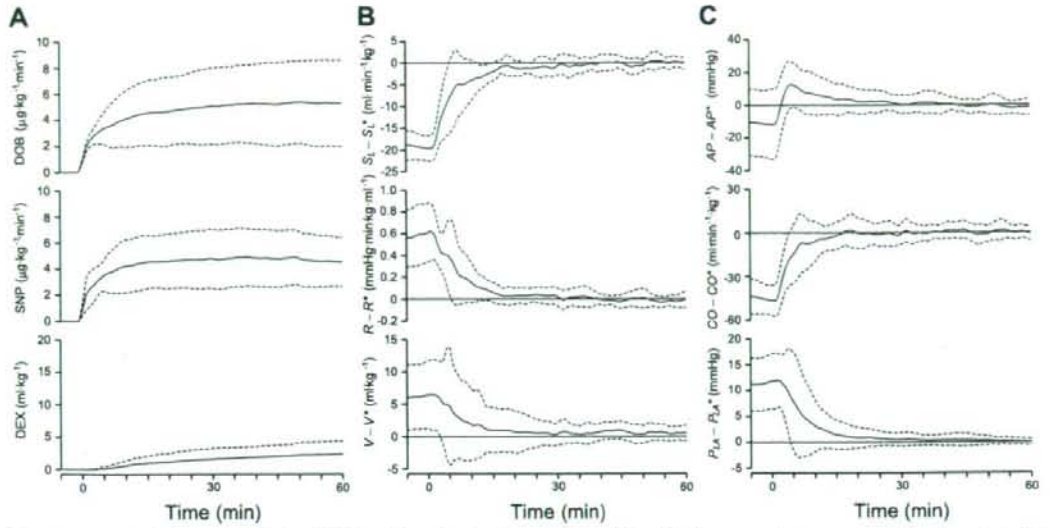

Fig. 5. Time courses of infusion rates of Dob and SNP, and cumulated volume of infused Dex (*A*), differences between measured and target cardiovascular parameters (*B*), and differences between measured and target hemodynamic variables (*C*) averaged for 12 dogs during closed-loop control of hemodynamics. Data are expressed as mean (solid line) ± SD (broken line). As the differences between measured and target parameters converged to the zero lines, the differences between measured and target hemodynamic variables also converged to the zero lines and remained at those levels.

respectively. The average standard deviations from the target values were small for AP [4.4 mmHg (SD 2.6)], CO [5.4 ml·min^{-1}·kg^{-1} (SD 2.4)] and Pla [0.8 mmHg (SD 0.6)]. In case of severe hypotension, restoring normal AP should be done within a few minutes to prevent cerebral ischemia. Four of 12 dogs exhibited severe hypotension [AP, 67 mmHg (SD 6)]. In these animals, AP* [95 mmHg (SD 4)] was attained within 4 min [mean 2.8 min (SD 0.7)]. Hemodynamic data before, during, and after the closed-loop control of hemodynamics are summarized in Table 3. After the system was turned off, AP, CO, and Pla gradually returned to their precontrol levels in 11 animals. In one animal, however, progressive hypotension followed by intractable ventricular fibrillation occurred ~3 min after the system was turned off.

In two dogs (*group 2*), AP, CO, and Pla were controlled with reasonable stability over a longer periods of time (100–150 min). Standard deviations from target values were small for AP (3.9–7.8 mmHg), CO (2.7–6.6 ml·min^{-1}·kg^{-1}), and Pla (0.7–2.5 mmHg).

Table 3. *Hemodynamic data before, during, and after the closed-loop control of hemodynamics*

	Before (n = 12)	During (n = 12)	After (n = 11)
HR, beats/mm	147.4 (26.8)	149.4 (25.0)	135.7 (25.2)†‡
AP, mmHg	86.7 (22.4)	97.0 (7.4)	75.2 (21.1)‡
CO, ml·min^{-1}·kg^{-1}	53.7 (14.6)	96.7 (5.3)†	53.5 (8.6)‡
Pla, mmHg	21.8 (5.5)	10.8 (1.2)†	18.5 (3.4)‡
Pra, mmHg	6.9 (1.8)	4.4 (0.9)†	7.4 (2.2)‡
S_L, ml·min^{-1}·kg^{-1}	14.3 (4.0)	32.7 (2.6)†	15.1 (2.9)‡
R, mmHg·min·ml^{-1}·kg	1.5 (0.3)	1.0 (0.1)†	1.3 (0.4)*‡
V, ml/kg	34.2 (4.9)	28.5 (2.3)†	34.0 (5.4)‡

Values are means (SD). *$P < 0.05$, †$P < 0.01$ vs. Before; ‡$P < 0.01$ vs. During.

DISCUSSION

To the best of our knowledge, the automated drug delivery system we have developed is the first to successfully control AP, CO, and Pla simultaneously with reasonably good accuracy and stability. In a canine model of acute heart failure, our system automatically normalizes AP, CO, and Pla and maintains the levels stably within the desired ranges. Therefore, our system is potentially useful in the management of patients with acute decompensated heart failure.

Previous Closed-Loop Systems Controlling Hemodynamic Variables

Several previous systems have attempted to control two hemodynamic variables simultaneously (18, 26, 27). However, it is difficult to expand them to closed-loop control of the overall hemodynamics.

Voss et al. (26) and Yu et al. (27) reported closed-loop systems to control AP and CO using inotropes and vasodilators in dogs. In these systems, all possible input-output relations between drug infusion and the response of the controlled variable have to be estimated; namely, inotrope-AP, inotrope-CO, vasodilator-AP, and vasodilator-CO relations. The reason for this is that these drugs affect AP and CO simultaneously to almost the same degree. If this approach is applied to simultaneous control of AP, CO, and Pla, at least nine input-output relations have to be estimated, because at least three drugs are required to independently control the three variables. This would make the system extremely complicated and therefore be practically unfeasible.

In addition, the input-output relations must be estimated online in individual animals to tune the drug controllers. The reason for this is that the relations differ widely between animals and within animal over time. Even the direction of the

output response can change. For example, CO usually increases in response to SNP infusion in subjects with failing hearts but may also decrease in subjects with preserved cardiac function (23, 26). In the closed-loop system of Voss et al., such estimation induced unacceptably large fluctuations in AP (26). The feasibility of such online estimation is questionable when drug infusion rates are allowed to vary simultaneously because of the difficulty to differentiate between drug effects. To avoid this problem, Hoeksel et al. (18) allowed only one drug to be varied at a time, whereas other drugs were kept constant in closed-loop control of AP and pulmonary arterial pressure during cardiac surgery. However, their adjustments of volume supplementation or dobutamine infusion were manual. Their system did not completely automate the control of hemodynamics.

Characteristics of Our System

Our system controls the cardiovascular parameters characterizing the integrated CO curve, venous return surface, and arterial resistance and as a result achieves target values for hemodynamic variables. Compared with previous systems, our system may appear to adopt a rather roundabout approach. Our concept is that controlling the cardiovascular parameters is physiologically more rational, because it is equivalent to directly controlling the mechanical determinants of circulation. As indicated by Guyton et al. (16, 17), when the mechanics of the circulation are considered, the hemodynamic variables such as AP, CO, and atrial pressures are the effects, or dependent variables. Blood volume and the mechanical properties of the heart and vasculature, such as heart rate, ventricular contractility, and vascular resistance, are the causes, or independent variables. The integrated CO curve and venous return surface display these properties through the relationship between the flow and atrial pressures (24, 25). The total artificial heart control system developed by Abe et al. (1) adjusted its output in accordance with the vascular conductance (1/resistance) and AP, thereby achieving appropriate response to peripheral metabolic demands and avoiding hemodynamic abnormalities exhibited by other total artificial heart control systems. Their results also suggest that it is essential to consider the mechanical determinant of circulation for the control of the hemodynamic variables.

Our approach is advantageous from the perspective of control engineering. The three drug controllers (Fig. 2*A*) are designed on the basis of only four input-output relations between the drug infusion and the response of the controlled parameter; namely, Dob-S_L, SNP-R, Dex-V, and Fur-V (Fig. 3). We also found that Dob decreases R and increases V, and SNP increases S_L and decreases V (data not shown), which are compatible with previous studies (7, 22, 23). If these secondary effects induce significant interactions among the three closed loops, additional controllers would be needed to compensate for the interactions (4). However, our results indicate that these secondary effects are small enough to be compensated by the three drug controllers, and additional controllers are not necessary. The fact that the three closed loops are effectively decoupled drastically simplifies the entire system. This also permits system operators to understand its behavior easily (4).

Although we fix the PI gain constants and the constants of if-then rules, controls of cardiovascular parameters are accurate and stable (Fig. 4*B*). There are interindividual differences in the response of the parameters to drug infusion (Fig. 3). There should also be intraindividual differences in the response over time. However, our results indicate that the three drug controllers effectively compensate for all of these differences and do not require adaptive tuning in individual animals as in the previous system. As long as each cardiovascular parameter responds sensitively to the corresponding agent, our system is able to achieve target values for all the parameters, thereby achieving target hemodynamic variables.

Our system explicitly quantifies cardiac pump function, preload, and afterload, thereby controlling the overall hemodynamics. We believe that this unique feature of our system is intuitively appealing and is acceptable to clinicians.

Clinical Application of Our System

Our system will reduce the stress and work imposed on physicians and nurses who are managing patients with unstable hemodynamic conditions. These personnel will be able to spend more time on other patient-related activities, thereby improving the quality of patient care (10, 11). We believe that the closed-loop control of overall hemodynamics can extend the improvement in postoperative outcome demonstrated by Chitwood et al. (10) to various aspects of clinical cardiology or cardiac surgery.

In clinical settings, multisystem disorders such as renal disease, anemia, and diabetes may affect the performance of our system. Renal disease can weaken the response of V to the infusion of Fur. The hemodynamic changes in anemia include increased preload and reduced arterial resistance as compensatory mechanisms for the reduced oxygen-carrying capacity of the blood (8). These changes may affect the control of V and R by our system. In patients with diabetic cardiomyopathy, the sensitivity of S_L to Dob infusion may be reduced (5). Drugs prescribed before hospitalization such as β-blockers, or used during hospitalization such as morphine may also affect the performance of our system. Chronic β-adrenergic blockade can weaken the sensitivity of S_L to Dob infusion (2). Administration of morphine may change the response of V and R to the drugs infused (15). We must clarify these effects on the performance of our system as thoroughly as possible before our system can be considered for clinical application.

In the routine clinical environment, CO, and pulmonary artery occlusion pressure, a substitute for Pla, are measured intermittently with a Swan-Ganz catheter. For clinical application of our system, it is a prerequisite to monitor these variables continuously. Several methods have been developed to continuously monitor CO or the pulmonary artery occlusion pressure (6, 12). Integrating these methods into our system would bring the clinical application of our system closer to reality.

Limitations

All the experiments of this study were conducted in anesthetized, open-chest dogs. Anesthesia and surgical trauma affect the cardiovascular system significantly. Whether the present system is efficacious in conscious, closed-chest animals (including humans) remains to be seen.

We parameterized the integrated cardiac output curve and the venous return surface using *Eqs. A1*, *A2*, and *A4* (24, 25). Even if the actual curve or surface deviate slightly from those

estimated by these equations, our system compensates such deviations by the negative feedback mechanism. However, we did not confirm whether the estimation works well outside the physiological ranges of Pla and Pra, particularly under low atrial pressures (24, 25). The efficacy of our system in such conditions remains to be evaluated.

Our system controls R with vasodilators only and lacks a controller to increase R with vasoconstrictors. This will not be a major problem because the pathophysiology of acute heart failure is characterized by excessive vasoconstriction due to enhanced activity of sympathetic and renin-angiotensin systems (19). Vasoconstrictor control is necessary, however, for the management of patients with excessive vasodilatation, such as those in septic shock (21).

In this study, control of S_L was accurate and stable. However, it would be impossible to restore S_L pharmacologically if S_L is more severely depressed than those seen in this study as in the case of more diffuse myocardial disease or superimposed coronary artery disease. We must clarify in future studies to what magnitude of S_L depression can our system restore it reliably. In addition, how to use our system with mechanical circulatory support such as the intra-aortic balloon pump in case of the severe S_L depression remains to be established.

In the present design, if S_L is unable to respond to the infusion of Dob, the system will automatically increase the infusion rate of Dob owing to its negative feedback mechanism. This would be problematic especially in case of arrhythmia, which is a serious noise in the closed-loop control of S_L. If not appropriately suppressed, frequent premature ventricular contractions or ventricular tachycardia will depress S_L owing to disorganized ventricular contraction. In response to the depressed S_L, the system automatically increases the infusion rate of dobutamine. This could further exacerbate the arrhythmia, thus leading to a vicious cycle and collapse of the hemodynamics. To prevent such malfunction, a smart "sensor" that will filter these unwanted artifacts should be included in our system.

In the present study, we recorded only the urine volume. Measurement of urine flow and sodium excretion is essential to evaluate renal function, which is a very important prognostic indicator in patients with acute decompensated heart failure (14). It would be desirable to add the monitoring of these parameters to our system to improve the quality of patient care.

In conclusion, by directly controlling the mechanical determinants of circulation, our automated drug delivery system allows simultaneous control of AP, CO, and Pla with reasonable accuracy and stability and is potentially a powerful clinical tool for the management of patients with acute decompensated heart failure.

APPENDIX A

Parameters of Integrated Cardiac Output Curve, Venous Return Surface, and Arterial Resistance

We parameterized the integrated CO curve, the venous return surface and the systemic arterial resistance on the basis of previous studies (24, 25). In the integrated CO curve, CO ($ml \cdot min^{-1} \cdot kg^{-1}$) is closely related to Pla (mmHg) by the following formula (24):

$$CO = S_L \times [\ln(Pla - 2.03) + 0.80] \quad (A1)$$

and CO to Pra (mmHg) as follows:

$$CO = S_R \times [\ln(Pra - 1.0) + 0.88] \quad (A2)$$

S_L and S_R ($ml \cdot min^{-1} \cdot kg^{-1}$) are parameters representing the preload sensitivity of CO, i.e., the pumping ability of the left and right heart, respectively. These relations are consistent among different animals (24). In a preliminary study, we found that the ratio of S_R to S_L (α) remains fairly constant during infusion of dobutamine (data not shown). This suggests that once we know α, we can predict S_R in relation to a known change in S_L. Therefore we used S_L to parameterize the integrated CO curve. S_L can be calculated from CO and Pla by rewriting *Eq. A1* as follows:

$$S_L = CO/[\ln(Pla - 2.03) + 0.80] \quad (A3)$$

The venous return surface can be mathematically expressed by the following formula (25):

$$CO_V = V/0.129 - 19.61Pra - 3.49Pla \quad (A4)$$

V (ml/kg) is total stressed blood volume, and CO_V ($ml \cdot min^{-1} \cdot kg^{-1}$) is integrated venous return from systemic and pulmonary circulations. This relationship is also consistent among different animals (25). We used V to parameterize the venous return surface. V can be calculated from CO (= CO_V), Pla, and Pra by rewriting *Eq. A4* as follows:

$$V = (CO + 19.61Pra + 3.49Pla) \times 0.129 \quad (A5)$$

We parameterized the systemic arterial resistance (R) ($mmHg \cdot ml^{-1} \cdot min \cdot kg$) by the following formula:

$$R = (AP - Pra)/CO \quad (A6)$$

APPENDIX B

Determination of Target Parameters

On the basis of AP*, CO*, and Pla*, our system determines S_L*, V*, and R* as follows: S_L* is calculated by substituting CO* and Pla* into *Eq. A3*. By substituting baseline CO, Pla, and Pra into *Eqs. A1* and *A2*, baseline S_L and S_R are calculated to determine α. S_R (S_R*) corresponding to S_L* is predicted as:

$$S_R^* = \alpha \cdot S_L^* \quad (B1)$$

From *Eq. A2* and *B1*, target Pra (Pra*) is predicted as:

$$Pra^* = \exp[(CO^*)/(S_R^*) - 0.88] + 1.0 \quad (B2)$$

By substituting CO*, Pla*, and Pra* into *Eq. A5*, V* can be determined. By substituting AP*, CO*, and Pra* into *Eq. A6*, R* can be calculated.

GRANTS

This study was supported by Grant-in-Aid for Young Scientists (B) (16700379) from the Ministry of Education, Culture, Sports, Science and Technology, by Health and Labour Sciences Research Grants for Research on Medical Devices for Analyzing, Supporting and Substituting the Function of Human Body (H15-physi-001) from the Ministry of Health Labour and Welfare of Japan, and by the Program for Promotion of Fundamental Studies in Health Science of the National Institute of Biomedical Innovation. This study was also conducted as a part of "Ground-based Research Announcement for Space Utilization" promoted by Japan Space Forum.

REFERENCES

1. **Abe Y, Chinzei T, Mabuchi K, Snyder AJ, Isoyama T, Imanishi K, Yonezawa T, Matsuura H, Kouno A, Ono T, Atsumi K, Fujimasa I, and Imachi K.** Physiological control of a total artificial heart: conductance- and arterial pressure-based control. *J Appl Physiol* 84: 868–876, 1998.
2. **Antman EM, Anbe DT, Armstrong PW, Bates ER, Green LA, Hand M, Hochman JS, Krumholz HM, Kushner FG, Lamas GA, Mullany CJ, Ornato JP, Pearle DL, Sloan MA, and Smith SC Jr; American College of Cardiology; American Heart Association; Canadian Car-**

diovascular Society. ACC/AHA guidelines for the management of patients with ST-elevation myocardial infarction—executive summary. A report of the American College of Cardiology/American Heart Association Task Force on Practice Guidelines (Writing Committee to revise the 1999 guidelines for the management of patients with acute myocardial infarction). *J Am Coll Cardiol* 44: 671–719, 2004.

3. **Arakawa M, Jerome EH, Enzan K, Grady M, and Staub NC.** Effects of dextran 70 on hemodynamics and lung liquid and protein exchange in awake sheep. *Circ Res* 67: 852–861, 1990.
4. **Astrom KJ and Hagglund T.** *PID Controller: Theory, Design, and Tuning* (2nd ed.). Research Triangle Park, NC: Instrument Society of America, 1995, p. 59–199.
5. **Atkins FL, Dowell RT, and Love S.** β-Adrenergic receptors, adenylate cyclase activity, and cardiac dysfunction in the diabetic rat. *J Cardiovasc Pharmacol* 7: 66–70, 1985.
6. **Bein B, Worthmann F, Tonner PH, Paris A, Steinfath M, Hedderich J, and Scholz J.** Comparison of esophageal Doppler, pulse contour analysis, and real-time pulmonary artery thermodilution for the continuous measurement of cardiac output. *J Cardiothorac Vasc Anesth* 18: 185–189, 2004.
7. **Binkley PF, Murray KD, Watson KM, Myerowitz PD, and Leier CV.** Dobutamine increases cardiac output of the total artificial heart. Implications for vascular contribution of inotropic agents to augmented ventricular function. *Circulation* 84: 1210–1215, 1991.
8. **Chapler CK and Cain SM.** The physiologic reserve in oxygen carrying capacity: studies in experimental hemodilution. *Can J Physiol Pharmacol* 64: 7–12, 1986.
9. **Chien KL, Hrones JA, and Reswick JB.** On the automatic control of generalized passive systems. *Trans ASME* 74: 175–185, 1952.
10. **Chitwood WR Jr, Cosgrove DM III, and Lust RM.** Multicenter trial of automated nitroprusside infusion for postoperative hypertension. Titrator Multicenter Study Group. *Ann Thorac Surg* 54: 517–522, 1992.
11. **Cosgrove DM III, Petre JH, Waller JL, Roth JV, Shepherd C, and Cohn LH.** Automated control of postoperative hypertension: a prospective, randomized multicenter study. *Ann Thorac Surg* 47: 678–682, 1989.
12. **DeBoisblanc BP, Pellett A, Johnson R, Champagne M, McClarty E, Dhillon G, and Levitzky M.** Estimation of pulmonary artery occlusion pressure by an artificial neural network. *Crit Care Med* 31: 261–266, 2003.
13. **Forrester JS, Diamond G, Chatterjee K, and Swan HJ.** Medical therapy of acute myocardial infarction by application of hemodynamic subsets (first of two parts). *N Engl J Med* 295: 1356–1362, 1976.
14. **Gottlieb SS, Abraham W, Butler J, Forman DE, Loh E, Massie BM, O'Connor CM, Rich MW, Stevenson LW, Young J, and Krumholz HM.** The prognostic importance of different definitions of worsening renal function in congestive heart failure. *J Card Fail* 8: 136–141, 2002.
15. **Greenberg S, McGowan C, Xie J, and Summer WR.** Selective pulmonary and venous smooth muscle relaxation by furosemide: a comparison with morphine. *J Pharmacol Exp Ther* 270: 1077–1085, 1994.
16. **Guyton AC.** Determination of cardiac output by equating venous return curves with cardiac response curves. *Physiol Rev* 35: 123–129, 1955.
17. **Guyton AC, Coleman TG, and Granger HJ.** Circulation: overall regulation. *Annu Rev Physiol* 34: 13–46, 1972.
18. **Hoeksel SA, Blom JA, Jansen JR, Maessen JG, and Schreuder JJ.** Automated infusion of vasoactive and inotropic drugs to control arterial and pulmonary pressures during cardiac surgery. *Crit Care Med* 27: 2792–2798, 1999.
19. **Johnson W, Omland T, Hall C, Lucas C, Myking OL, Collins C, Pfeffer M, Rouleau JL, and Stevenson LW.** Neurohormonal activation rapidly decreases after intravenous therapy with diuretics and vasodilators for class IV heart failure. *J Am Coll Cardiol* 39: 1623–1629, 2002.
20. **Kaplan JA and Guffin AV.** Treatment of perioperative left ventricular failure. In: *Cardiac Anesthesia* (3rd ed.), edited by Kaplan JA. Philadelphia, PA: Saunders, 1993, p. 1058–1094.
21. **Martin C, Viviand X, Arnaud S, Vialet R, and Rougnon T.** Effects of norepinephrine plus dobutamine or norepinephrine alone on left ventricular performance of septic shock patients. *Crit Care Med* 27: 1708–1713, 1999.
22. **Ogilvie RI and Zborowska-Sluis D.** Effects of nitroglycerin and nitroprusside on vascular capacitance of anesthetized ganglion-blocked dogs. *J Cardiovasc Pharmacol* 18: 574–580, 1991.
23. **Pouleur H, Covell JW, and Ross J Jr.** Effects of nitroprusside on venous return and central blood volume in the absence and presence of acute heart failure. *Circulation* 61: 328–337, 1980.
24. **Uemura K, Kawada T, Kamiya A, Aiba T, Hidaka I, Sunagawa K, and Sugimachi M.** Prediction of circulatory equilibrium in response to changes in stressed blood volume. *Am J Physiol Heart Circ Physiol* 289: H301–H307, 2005.
25. **Uemura K, Sugimachi M, Kawada T, Kamiya A, Jin Y, Kashihara K, and Sunagawa K.** A novel framework of circulatory equilibrium. *Am J Physiol Heart Circ Physiol* 286: H2376–H2385, 2004.
26. **Voss GI, Katona PG, and Chizeck HJ.** Adaptive multivariable drug delivery: control of arterial pressure and cardiac output in anesthetized dogs. *IEEE Trans Biomed Eng* 34: 617–623, 1987.
27. **Yu C, Roy RJ, Kaufman H, and Bequette BW.** Multiple-model adaptive predictive control of mean arterial pressure and cardiac output. *IEEE Trans Biomed Eng* 39: 765–778, 1992.

Acta Physiol 2007, 191, 275–284

Characterization of ouabain-induced noradrenaline and acetylcholine release from *in situ* cardiac autonomic nerve endings

T. Yamazaki,[1] T. Akiyama,[1] H. Kitagawa,[1] F. Komaki,[1] H. Mori,[1] T. Kawada,[2] K. Sunagawa[2] and M. Sugimachi[2]

1 *Department of Cardiac Physiology, National Cardiovascular Center Research Institute, Suita, Osaka, Japan*

2 *Department of Cardiovascular Dynamics, National Cardiovascular Center Research Institute, Suita, Osaka, Japan*

Received 11 January 2007, revision requested 28 March 2007, revision received 29 May 2007, accepted 30 June 2007

Correspondence: T. Yamazaki, Department of Cardiac Physiology, National Cardiovascular Center Research Institute, 5-7-1 Fujishirodai, Suita, Osaka 565, Japan. E-mail: yamazaki@ri.ncvc.go.jp

Abstract

Aim: Although ouabain modulates autonomic nerve ending function, it is uncertain whether ouabain-induced releasing mechanism differs between *in vivo* sympathetic and parasympathetic nerve endings. Using cardiac dialysis, we examined how ouabain induces neurotransmitter release from autonomic nerve ending.

Methods: Dialysis probe was implanted in left ventricle, and dialysate noradrenaline (NA) or acetylcholine (ACh) levels in the anaesthetized cats were measured as indices of neurotransmitter release from post-ganglionic autonomic nerve endings.

Results: Locally applied ouabain (100 μM) increased in dialysate NA or ACh levels. The ouabain-induced increases in NA levels remained unaffected by cardiac sympathetic denervation and tetrodotoxin (Na^+ channel blocker, TTX), but the ouabain-induced increases in ACh levels were attenuated by TTX. The ouabain-induced increases in NA levels were suppressed by pretreatment with desipramine (NA transport blocker) and augmented by reserpine (vesicle NA transport blocker). In contrast, the ouabain-induced increases in ACh levels remained unaffected by pretreatment with hemicholinium-3 (choline transport blocker) but suppressed by vesamicol (vesicle ACh transport blocker). The ouabain-induced increases in NA levels were suppressed by pretreatment with ω-conotoxin GVIA (N-type Ca^{2+} channel blocker), verapamil (L-type Ca^{2+} channel blocker) and TMB-8 (intracellular Ca^{2+} antagonist). The ouabain-induced increases in ACh levels were suppressed by pretreatment with ω-conotoxin MVIIC (P/Q-type Ca^{2+} channel blocker), and TMB-8.

Conclusions: Ouabain-induced NA release is attributable to the mechanisms of regional exocytosis and/or carrier-mediated outward transport of NA, from stored NA vesicle and/or axoplasma, respectively, while the ouabain-induced ACh release is attributable to the mechanism of exocytosis, which is triggered by regional depolarization. At both sympathetic and parasympathetic nerve endings, the regional exocytosis is because of opening of calcium channels and intracellular calcium mobilization.

Keywords acetylcholine, Ca^{2+} channels, cat, microdialysis, Na^+,K^+-ATPase, noradrenaline.

 doi: 10.1111/j.1748-1716.2007.01749.x

It is generally accepted that ouabain modulates autonomic nerve function by inhibition of membrane Na^+,K^+-ATPase (Gillis & Quest 1979). This neuronal modulatory effect was mainly reported with *in vitro* sympathetic (Sweadner 1985), parasympathetic nerve endings (Satoh & Nakazato 1992, Gomez *et al.* 1996) and adrenal glands (Haass *et al.* 1997). Furthermore, ouabain-induced modulatory effect was reported with *in vitro* studies on motor endplate (Vyskocil & Illes 1977, Zemkova *et al.* 1990). From these *in vitro* studies, several mechanisms are presently suggested to induce release of neurotransmitter from the nerve endings. However, it is uncertain whether the manner of modulation differs between *in vivo* sympathetic and parasympathetic nerve endings. A major concern is whether ouabain induces a brisk increase in neurotransmitter efflux (spontaneous neurotransmitter release). Kranzhöfer *et al.* (1991) reported that ouabain-induced spontaneous noradrenaline (NA) release from sympathetic nerve endings. On the other hand, ouabain-induced spontaneous acetylcholine (ACh) release was reported *in vitro* studies using synaptosomes (Satoh & Nakazato 1992). No reports have described *in vivo* spontaneous ACh release evoked by ouabain. Further, a second issue is at which site ouabain induces neurotransmitter release: stored vesicle or axoplasma (Haass *et al.* 1997). NA and ACh release have been reported in stored vesicles and/or the axoplasma. It is uncertain, however, which site induces the predominant neurotransmitter release evoked by ouabain *in vivo*. Furthermore, the mechanisms underlying the neurotransmitter release evoked by ouabain remain unclear. Neuronal effects of ouabain have been attributed to the inhibitory action upon Na^+,K^+-ATPase and transmembrane sodium pump (Haass *et al.* 1997). As a consequence of the reduced sodium gradient at the plasma membrane, two possible mechanisms have been proposed to induce NA release from nerve endings; (i) carrier-mediated reversed NA transport, and (ii) Ca^{2+}-dependent exocytotic NA release. The manner and mechanisms of NA efflux have been extensively studied and accepted *in vivo* in isolated tissues (Sweadner 1985, Haass *et al.* 1997). However, it remains unclear whether these assumptions are valid in the cardiac sympathetic or parasympathetic nerve endings *in vivo*.

Cardiac dialysis technique in combination with highly sensitive measurement of NA or ACh has offered a powerful method for detecting the low level of dialysate NA or ACh obtained from the myocardial space (Akiyama *et al.* 1991, 1994). We demonstrated that dialysate NA or ACh levels were affected by local administration of pharmacological agents through dialysis probes, indicating that changes in dialysate NA or ACh levels reflect NA or ACh output from cardiac postganglionic sympathetic or parasympathetic nerve endings (Yamazaki *et al.* 1997, Kawada *et al.* 2001) respectively. Using dialysis technique, ouabain can be administered locally and it is possible to monitor NA or ACh output following locally applied ouabain (Yamazaki *et al.* 2001). Furthermore, comparison of the dialysate NA response in the presence and absence of neuronal agents can differentiate carrier-mediated NA release from calcium dependent exocytotic NA release (Yamazaki *et al.* 1997). With locally applied neuronal blockers, we examined the mechanisms and the sites underlying NA or ACh release evoked by ouabain.

Methods

Animal preparation

Adult cats were anaesthetized with pentobarbital sodium (30–35 mg kg^{-1} i.p.). The level of anaesthesia was maintained with a continuous intravenous infusion of pentobarbital sodium (1–2 mg kg^{-1} h^{-1}). The animals were intubated and ventilated with room air mixed with oxygen. Body temperature was maintained using a heated pad and lamp. All protocols were performed in accordance with the National Cardiovascular Center Research Institute Animal Care Ethics Committee guidelines that were in strict compliance with the NIH Guide for the Care and Use of Laboratory Animals. Electrocardiogram and mean arterial pressure were simultaneously monitored with a data recorder. The sixth rib on the left side was resected to expose the heart. With a fine guiding needle, one or two dialysis probes for dialysate sampling were implanted in the mid wall of the anterolateral region of the left ventricle. Heparin (100 U kg^{-1}) was administered after implantation of the dialysis probe and a maintenance dose was given every hour thereafter.

Dialysis technique

The material and properties of the dialysis probe were described previously (Akiyama *et al.* 1991, 1994). Briefly, we designed a transverse dialysis probe. Both ends of a dialysis fibre (13 mm length, 0.31 mm o.d. and 0.2 mm i.d.; PAN-1200, 50 000 molecular weight cutoff, Asahi Chemical, Tokyo, Japan) were connected and glued to polyethylene tubes (25 cm length, 0.5 mm o.d. and 0.2 mm i.d.). The dialysate NA or ACh levels were measured in separate animals. For the measurement of dialysate NA, the dialysis probe was perfused with Ringer's solution at 10 μL min^{-1}. Sampling periods were 2 min in duration (one sample volume = 20 μL), which was the minimum period necessary to collect sufficient NA for satisfactory measurement. For the measurement of dialysate ACh, Ringer's solution containing eserine (choline esterase

 doi: 10.1111/j.1748-1716.2007.01749.x

inhibitor, 100 μM) was perfused at 2 μL min^{-1} and sampling periods were 15 min in duration. Dialysate sampling was started 120 min after probe implantation, when the dialysate NA or ACh concentration had reached a steady level. Each sample was collected in a microtube containing 0.1 N HCl or phosphate buffer to prevent oxidation. The dead-space volume between the dialysis and sample tube was measured. Taking this dead-space into account, samples were obtained.

Experimental protocols

In our previous study, we demonstrated that the dialysate NA or ACh levels reflect cardiac neuronal NA or ACh disposition at the nerve endings (Yamazaki *et al.* 1997, Kawada *et al.* 2001). Therefore, in the present study, we obtained dialysate samples and measured the dialysate NA or ACh levels as an index of NA or ACh output from post-ganglionic sympathetic or parasympathetic nerve endings respectively. Generally two mechanisms and sites are proposed to induce NA and ACh release from nerve endings: exocytotic (quantum) release from the stored vesicle and non-exocytotic (non-quantum) release from the axoplasma. The present studies were designed to clarify whether ouabain-induced NA or ACh efflux are affected by local administration of pharmacological agents that modify experimental conditions.

Protocol 1: Time courses of dialysate NA and ACh levels during local administration of ouabain. We examined the time course of dialysate NA and ACh levels during local administration of ouabain (100 μM). Ouabain was administered for 60 min. Dialysate NA levels were measured before and at 10-min intervals during ouabain administration. Dialysate ACh levels were collected in consecutive 15-min sampling periods.

Protocol 2: Influence of nerve transection and Na^+ channels on dialysate NA or ACh response evoked by ouabain. To test whether ouabain modulated central-mediated exocytotic neurotransmitter release, we examined the time course of ouabain-induced dialysate NA and ACh levels after transection of stellate ganglia or cervical parasympathetic nerve tract. For cardiac sympathetic denervation, the region of the stellate ganglia was exposed through the intercostal space, and bilateral transection of stellate ganglia was performed. After cardiac sympathetic denervation, heart rate response to carotid occlusion was blunted. In separate cats, cervical vagotomy was performed. We started dialysate sampling at 120 min after surgical interruption and ouabain-induced NA or ACh efflux was examined. Furthermore, to examine involvement of deporalization on NA or ACh release, ouabain-induced NA or ACh efflux was measured with addition of tetrodotoxin (TTX, 10 μM) through the dialysis probe. At 60 min after the beginning of TTX administration, we started the control sampling and examined the ouabain-induced NA or ACh response.

Protocol 3: Influence of NA-, ACh- and choline transporters on dialysate NA or ACh response evoked by ouabain. To test whether ouabain-induced neurotransmitter efflux was derived from axoplasma or stored vesicle, ouabain-induced NA or ACh efflux was examined with local administration of pharmacological agents, which affected the transport and content of neurotransmitter at the nerve endings. Membrane carrier-mediated NA transport was blocked by local administration of desipramine, whereas vesicular NA import was blocked by local administration of reserpine. In either case, ouabain-induced NA efflux was examined with the addition of desipramine (100 μM) or reserpine (10 μM) through the dialysis probe. The dosage of agent-administration was decided after referring to the previous studies (Akiyama *et al.* 1994, Yamazaki *et al.* 1997). Membrane carrier-mediated choline transport was blocked by local administration of hemicholinium-3 (10 μM), whereas vesicular ACh import was blocked by local administration of vesamicol (10 μM) (Kawada *et al.* 2001). In either case, ouabain-induced ACh efflux was examined with the addition of hemicholinium-3 or vesamicol through the dialysis probe.

Protocol 4: Influence of Ca^{2+} transporter, channel, mobilization on dialysate NA or ACh response evoked by ouabain. To test the contention that ouabain-induced neurotransmitter efflux was modulated by changes in intracellular Ca^{2+} levels, the influence of Ca^{2+} transporter, channel, mobilization on the dialysate NA or ACh response evoked by ouabain was examined. We focused on the involvement of three types of voltage-dependent Ca^{2+} channel, the L- and N types in the NA release evoked by ouabain. Sixty minutes after starting local administration of verapamil (100 μM), or ω-conotoxin GVIA (10 μM), we measured the ouabain-induced NA response. Second, we examined the involvement of plasma membrane Na^+/Ca^{2+} exchanger in the NA release evoked by ouabain. The inhibitors of membrane Na^+/Ca^{2+} exchange (dechlorobezamil; 100 μM, or KB7943; 10 μM) were locally administered through the dialysis probe and the ouabain-induced NA response was measured. Third, we examined the involvement of intracellular Ca^{2+} level in the NA release evoked by ouabain. An intracellular Ca^{2+} antagonist [3,4,5-trimethoxybenzoic acid 8-(dietyl amino)-octyl ester (TMB-8)] blocks the efflux of calcium from intracellular calcium stores without affecting influx

 doi: 10.1111/j.1748-1716.2007.01749.x

(Wiedenkeller & Sharp 1984). TMB-8 (1 mM) was locally administered through the dialysis probe and ouabain-induced NA response was measured. A similar pharmacological intervention was performed and ouabain-induced ACh responses were measured. Sixty minutes after starting local administration of verapamil (100 μM), or ω-conotoxin GVIA (10 μM), ω-conotoxin MVIIC (10 μM), we measured the ouabain-induced ACh response. The inhibitor of membrane Na^+/Ca^{2+} exchange (KB7943; 10 μM) was locally administered through the dialysis probe and the ouabain-induced ACh response was measured. Third, an intracellular Ca^{2+} antagonist (TMB-8, 1 mM) was locally administered through the dialysis probe and ouabain-induced ACh response was measured.

Analytical procedure

Dialysate NA concentrations were measured by HPLC with electrochemical detection (HPLC-ECD; Eicom, Kyoto, Japan). An alumina procedure was performed to remove the interfering compounds from the dialysate. The detection limit was 50 fmol per injection. Dialysate ACh concentration was measured directly by another HPLC-ECD. The detection limit was 50 fmol per injection. Details of HPLC-ECD for the NA and ACh measurements have been described elsewhere (Akiyama *et al.* 1991, 1994).

At the end of each experiment, the cats were killed with an overdose of pentobarbital sodium, and the implant sites were checked to confirm that the dialysis probes had been implanted within the left ventricular myocardium. Statistical analysis of the data was performed by analysis of variance (ANOVA). Statistical significance was defined as $P < 0.05$. Values are presented as mean ± SE.

Results

Protocol 1: Time course of dialysate NA and ACh levels during local administration of ouabain

Although local administration of ouabain did not affect haemodynamic parameters including heart rate, mean arterial pressure and electrocardiogram, ouabain induced the efflux of NA. Figure 1 (upper panel) shows the time course of the dialysate NA levels during local administration of ouabain (100 μM). Dialysate NA level increased significantly from 0.18 ± 0.06 nmol L^{-1} at control to 2.39 ± 0.53 nmol L^{-1} at 10, 12.92 ± 1.39 nmol L^{-1} at 20 min and 14.79 ± 1.97 nmol L^{-1} at 30 min. Subsequently, a slow decline occurred but high dialysate NA levels were maintained during locally applied ouabain. Peak level of dialysate NA ranged from 20 to 30 min after the beginning of ouabain administration. Figure 1 (lower panel) shows the time course of the dialysate ACh levels during local administration of ouabain (100 μM). Dialysate ACh level increased significantly from 0.91 ± 0.05 nmol at control to 3.6 ± 0.60 nmol L^{-1} at 0–15, 8.1 ± 1.4 nmol L^{-1} at 15–30 min and 6.8 ± 1.25 nmol L^{-1} at 30–45 min. Peak level of dialysate ACh appeared at 15–30 min after the beginning of ouabain administration.

Protocol 2: Influence of denervation and TTX on dialysate NA and ACh responses evoked by ouabain

We sampled the dialysates over 60 min of ouabain administration. To compare ouabain-induced NA or ACh levels under various interventions, ouabain-induced dialysate NA or ACh levels were subtracted from the control values. The sum of relative changes in dialysate NA or ACh (the unit: Σnmol/L) was expressed as an index of total NA or ACh release evoked by ouabain. Figure 2 (upper panel) shows the total NA release evoked by ouabain when cardiac sympathetic nerves were either intact, transected, pretreated with TTX. The ouabain-induced total NA release did not differ among them. Figure 2 (lower panel) shows the total ACh release evoked by ouabain when cardiac parasympathetic nerves were either intact, transected, or pretreated with TTX. The ouabain-induced total ACh release did not differ between the intact cardiac parasympathetic nerve and denervated groups whereas addition of TTX significantly inhibited the total ACh release by approx. 57% of vehicle.

Protocol 3: Influence of transport blocking agents on dialysate NA and ACh responses evoked by ouabain

Figure 3 (upper panel) shows the total NA release evoked by ouabain among various pharmacological interventions. Pretreatment with reserpine caused significant augmentation of the ouabain-induced total NA release whereas pretreatment with desipramine caused significant suppression of the total NA release. Figure 3 (lower panel) shows the total ACh release evoked by ouabain among various pharmacological interventions. The ouabain-induced total ACh release did not differ between the intact and hemicholinium-3 pretreated groups whereas addition of vesamicol significantly inhibited the total ACh release by approx. 45% of vehicle.

Protocol 4: Influence of Ca^{2+} mobilization on dialysate NA and ACh responses evoked by ouabain

Figure 4 (upper panel) shows the total NA release evoked by ouabain among various Ca^{2+} interventions. The total NA release in the 60 min after administration

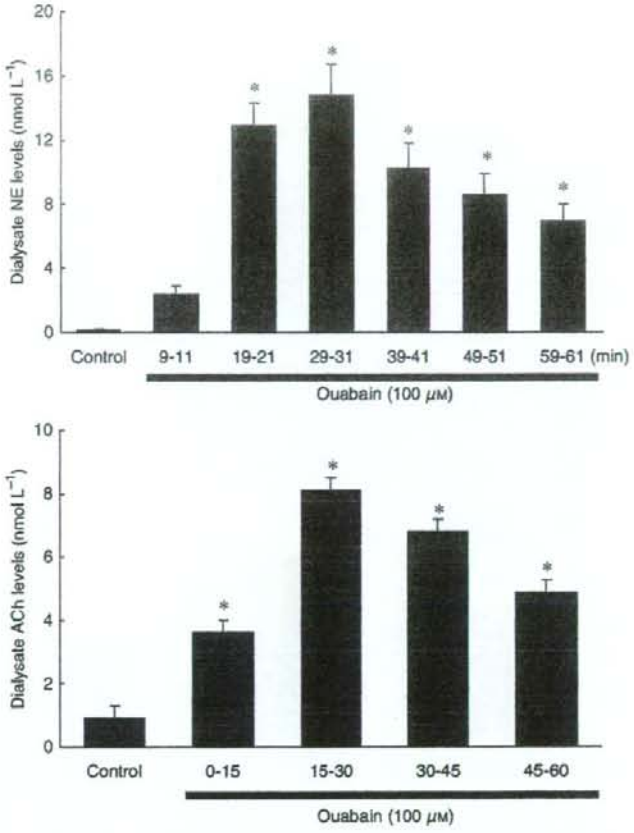

Figure 1 Upper panel: Time course of dialysate noradrenaline (NA) levels during local administration of ouabain (100 μM). Ouabain increased the dialysate NA levels. Subsequently, a slow decline occurred but high NA levels were maintained. Lower panel: Time course of dialysate acetylcholine (ACh) levels during local administration of ouabain (100 μM). Ouabain increased the dialysate ACh levels. Subsequently, a slow decline occurred but high ACh levels were maintained. Values are presented as the mean ± SE (for each column $n = 6$) $^*P < 0.05$ vs. control.

of ouabain was significantly suppressed by approx. 47% and 55% of vehicle by addition of verapamil and ω-conotoxin GVIA. Pretreatment with TMB-8 caused significant suppression of the ouabain-induced total NA release whereas pretreatment with neither KB-7943 nor dechlorobezamil altered the total NA release. Figure 4 (lower panel) shows the total ACh release evoked by ouabain among various Ca^{2+} interventions. The total ACh release in the 60 min after administration of ouabain was significantly suppressed by approx. 57% of vehicle by addition of ω-conotoxin MVIIC. Pretreatment with neither verapamil nor ω-conotoxin GVIA altered the total ACh release. Pretreatment with TMB-8 caused significant suppression of the ouabain-induced total ACh release whereas pretreatment with KB-7943 did not alter the total ACh release.

Discussion

The present study indicates that in an *in vivo* preparation, ouabain alone induced NA or ACh release from sympathetic or parasympathetic nerve endings respectively. This discussion addresses mainly similarities and differences in ouabain alone induced NA or ACh releasing sites and mechanisms.

Regional depolarization evoked by ouabain

At the post-ganglionic nervous endings, ouabain induced NA and ACh release. The transection of sympathetic or parasympathetic nerve did not affect the amount of NA or ACh release evoked by ouabain. After the transection of cardiac sympathetic or parasympathetic nerves, ouabain at 100 μM induced increases in dialysate NA or ACh levels, which were as much as those evoked by electrical stimulation of the autonomic nerve (Akiyama *et al.* 1994, Yamazaki *et al.* 1997). These data suggest that ouabain itself induces regional depolarization following exocytosis. In the case of locally administered ouabain, ouabain produced intracellular Na^+ accumulation evoked by the inhibition of Na^+,K^+-ATPase (McIvor & Cummings 1987).

 doi: 10.1111/j.1748-1716.2007.01749.x

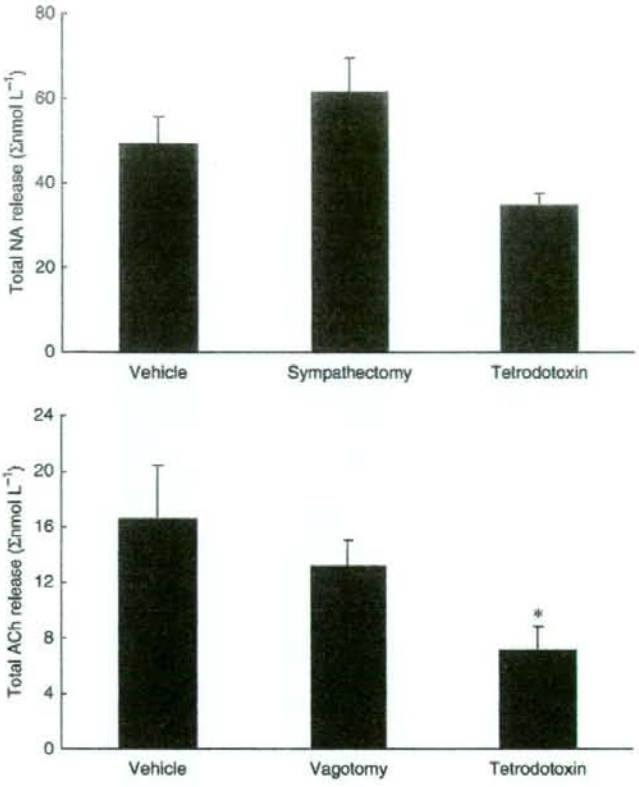

Figure 2 Upper panel: Ouabain-induced dialysate noradrenaline (NA) release in vehicle, cardiac sympathetic denervated and tetrodotoxin pretreated groups. Total NA release evoked by ouabain did not differ among the three groups. Lower panel: Ouabain-induced dialysate acetylcholine (ACh) release in vehicle, cardiac vagal denervated and tetrodotoxin pretreated groups. Total ACh release evoked by ouabain was suppressed by the pretreatment with tetrodotoxin. Values are presented as the mean ± SE (for each column $n = 6$). $^*P < 0.05$ vs. vehicle.

Regional depolarization may occur because of intracellular Na^+ accumulation (Calabresi *et al.* 1999, Dierkes *et al.* 2006). Similar finding was observed on motor endplate (Zemkova *et al.* 1990). Ouabain can increase the spontaneous ACh release by progressive decline in membrane potential when Na^+ pump is inhibited. If regional depolarization does indeed induce ACh or NA release via exocytosis from the stored vesicle, then pretreatment with TTX could inhibit this response. Local administration of TTX markedly inhibits ACh release whereas it only slightly inhibits the NA release evoked by ouabain. These results indicate that ouabain caused regional depolarization and exocytotic ACh release at the parasympathetic nerve endings. This conclusion is consistent with *in vitro* studies reported by Satoh & Nakazato (1992), and raises the question as to why TTX inhibited the ACh release but not the NA release evoked by ouabain. In the case of NA efflux evoked by ouabain, intracellular Na^+ accumulation may lead to a reduction in the Na^+ gradient between the intracellular and extracellular spaces. This reduced Na^+ gradient may cause carrier-mediated outward NA transport from axoplasma (Sharma *et al.* 1980). The threshold for intracellular Na^+ accumulation coupled to carrier-mediated outward NA transport might be lower than that for regional depolarization. Thus Na^+ accumulation coupled to regional depolarization may occur at the parasympathetic nerve endings but not at the sympathetic nerve endings.

The sites of neurotransmitter efflux evoked by ouabain

In general, two possible sites (the stored vesicle and axoplasma) were proposed to derive efflux of neurotransmitter at the nerve endings (Smith 1992, Vizi 1998). In the cholinergic nerve endings, a quantum amount of ACh was released from the stored vesicle via depolarization. Furthermore, a non-quantum amount of ACh seems to be leaked from the axoplasma without ACh transporter (Nikolsky *et al.* 1991). Local administration of vesamicol suppressed the ACh efflux evoked by ouabain. In contrast, local administration of hemicholinium-3 did not affect the ACh efflux evoked by ouabain. These data suggested that the ACh efflux was predominantly derived from the stored vesicle. This finding is consistent with the above-mentioned

Journal compilation © 2007 Scandinavian Physiological Society, doi: 10.1111/j.1748-1716.2007.01749.x

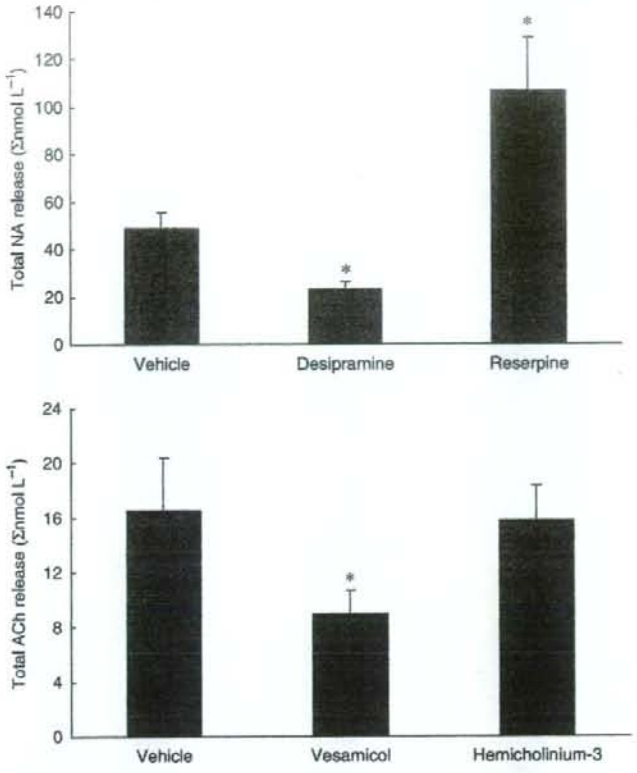

Figure 3 Upper panel: Ouabain-induced dialysate noradrenaline (NA) release among vehicle, desipramine and reserpine pretreated groups. Total NA release evoked by ouabain was suppressed by the pretreatment with desipramine and augmented by that with reserpine. Lower panel: Ouabain-induced dialysate acetylcholine (ACh) release in vehicle, vesamicol and hemicholinium-3 pretreated groups. Total ACh release evoked by ouabain was suppressed by the pretreatment with vesamicol. Values are presented as the mean ± SE (for each column $n = 6$). $^*P < 0.05$ vs. vehicle.

mechanism. Our data did not rule out the possibility of ACh efflux from the axoplasma. Vesamicol lowered the non-quantum ACh release by blocking the incorporated vesicle transporter in the terminal membrane (Edward *et al.* 1985). This involvement seems to be smaller than the involvement of ACh efflux from the stored vesicle.

Previous studies suggested that two different mechanisms (exocytosis and carrier-mediated outward transport) contributed to the amount of NA efflux evoked by ouabain (Kranzhöfer *et al.* 1991, Haass *et al.* 1997). The exocytotic NA release derived from the stored vesicle, whereas NA transporter carried out NA from the axoplasmic site via a reduced Na^+ gradient. However, it is uncertain which mechanism is predominantly involved in ouabain-induced NA efflux. To examine which site predominantly induced the neurotransmitter efflux evoked by ouabain, we administered vesicle and membranous amine transport blockers, which affected the neurotransmitter efflux evoked by ouabain. If NA efflux predominantly derives from the axoplasmic site, reserpine could increase axoplasmic NA level and augment the outward NA transport evoked by ouabain. Furthermore, as desipramine impairs carrier-mediated NA transport in both directions, desipramine could block NA efflux. NA release evoked by ouabain was augmented by local administration of reserpine but suppressed by desipramine. These data support the contention that ouabain-induced NA efflux is predominantly derived from the axoplasmic site.

Involvement of Ca^{2+} on ouabain-induced neurotransmitter efflux

Most *in vitro* studies suggested that ouabain somehow increases intracellular Ca^{2+} levels at the nerve endings and synaptosomes (Katsuragi *et al.* 1994, Casali *et al.* 1995, Wasserstrom & Aistrup 2005). Ouabain-induced intracellular Na^+ accumulation could evoke an elevation of intracellular Ca^{2+} level via Ca^{2+} channel opening (Katsuragi *et al.* 1994), Ca^{2+} release from internal stores (Nishio *et al.* 2004), and/or Na^+/Ca^{2+} exchange (Verbny *et al.* 2002). Thus, the elevation of intracellular Ca^{2+} may be associated with NA or ACh release from the autonomic nerve endings. At the parasympathetic nerve endings, neither verapamil nor ω-conotoxin GVIA

 doi: 10.1111/j.1748-1716.2007.01749.x